A MULTIPHASE CAHN-HILLIARD SYSTEM WITH MOBILITIES FOR THE SIMULATION OF WETTING

ELIE BRETIN, ROLAND DENIS, SIMON MASNOU, ARNAUD SENGERS, AND GARRY TERII

ABSTRACT. We propose in this paper a new multiphase Cahn–Hilliard model with doubly degenerate mobilities. We prove by matched asymptotic expansion that it approximates with a second order accuracy the multiphase surface diffusion flow with mobilities and surface tensions. To show that it is very well suited for numerical approximation, we propose a simple and efficient numerical scheme together with a very compact Matlab implementation. We illustrate with various numerical experiments the influence of mobility and surface tension coefficients. The second-order accuracy of our model, and its appropriateness for numerical implementation, makes it suitable for tackling notably difficult surface diffusion problems. In particular, we show that it can be used very effectively to simulate the wetting of thin liquid tubes even on rough solid supports without requiring nonlinear boundary conditions.

1. INTRODUCTION

The wetting or dewetting phenomenon describes the behavior of a liquid phase put in contact with a fixed solid surface. This paper is devoted to the phase field approximation of this phenomenon as a multiphasic surface diffusion flow with mobilities. Young [**?**] identified in 1805 the optimal shape of the liquid phase and proposed the following law for the contact angle θ between the liquid and the solid:

$$\cos(\theta) = \frac{\sigma_{SV} - \sigma_{LS}}{\sigma_{VL}},$$

where $\sigma_{SV}, \sigma_{LS}, \sigma_{VL}$ represent the surfaces tensions of the interfaces solid-vapor Γ_{SV}, liquid-solid Γ_{LS} and vapor-liquid Γ_{VL}, respectively. Mathematically, Young's law can be derived by minimizing the total energy in the solid-liquid-vapor system. Ignoring gravity, this total energy reads as

$$\mathcal{E} = \sigma_{SV}\mathcal{H}^{d-1}(\Gamma_{SV}) + \sigma_{LS}\mathcal{H}^{d-1}(\Gamma_{LS}) + \sigma_{VL}\mathcal{H}^{d-1}(\Gamma_{VL}).$$

which is a particular instance of the generic L-phase perimeter

$$P(\Omega_1, \dots, \Omega_L) = \frac{1}{2}\sum_{i,j=1}^{L} \sigma_{i,j}\mathcal{H}^{d-1}(\Gamma_{i,j}), \tag{1}$$

where $\{\Omega_1, \dots, \Omega_L\}$ is an open partition of an open bounded domain $\Omega \subset \mathbb{R}^d$ and, for all $i, j \in \{1, \dots, L\}$, $\Gamma_{i,j} = \bar{\Omega}_i \cap \bar{\Omega}_j \cap \Omega$ is the interface between phases i, j, and $\sigma_{i,j}$ is the surface tension along this interface. To ensure the lower semicontinuity of the L-phase perimeter, see [**?**, **?**, **?**], we assume that the surface tensions are positive, i.e. $\sigma_{i,j} > 0$, and satisfy the triangle inequality

$$\sigma_{i,j} + \sigma_{j,k} \geq \sigma_{i,k} \quad \text{for any } i, j, k,$$

The evolution of the physical system can then be approximated by a multiphasic surface diffusion flow. This motion can be viewed as the H^{-1} gradient flow of the energy (1) which

2020 *Mathematics Subject Classification.* 74N20, 35A35, 53E10, 53E40, 65M32, 35A15.

Key words and phrases. Phase field approximation, multiphase Cahn-Hilliard system, surface diffusion, degenerate mobilities, numerical approximation, wetting.

ensures its decay while maintaining locally the volume of each phase. In particular, the normal velocity V_{ij} at the interface Γ_{ij} reads as

$$\frac{1}{\nu_{ij}} V_{ij} = \sigma_{ij} \Delta_{\Gamma_{ij}(t)} H_{ij}(t),$$

where $H_{ij}(t)$ denotes the scalar mean curvature on $\Gamma_{ij}(t)$, $\Delta_{\Gamma_{ij}(t)}$ is the Laplace-Beltrami operator on the surface, and $\nu_{ij} > 0$ is the surface mobility coefficient. The above expression is the classical form of the velocity in this context, but it can be obviously rewritten to incorporate the degenerate no-motion case where $\nu_{ij} = 0$:

$$V_{ij} = \nu_{ij} \sigma_{ij} \Delta_{\Gamma_{ij}(t)} H_{ij}(t).$$

The simulation of wetting or dewetting requires $L = 3$ phases: the liquid phase Ω_L, the solid phase Ω_S and the vapor phase Ω_V. Moreover, as the surface tension coefficients $(\sigma_{LV}, \sigma_{SV}, \sigma_{SL})$ satisfy the triangle inequality, they form an additive set of coefficients, i.e. there exists three positive coefficients $\sigma_L, \sigma_S, \sigma_V$ such that

$$\sigma_{LV} = \sigma_L + \sigma_V, \quad \sigma_{SV} = \sigma_S + \sigma_V \text{ and } \quad \sigma_{SV} = \sigma_S + \sigma_V.$$

The surface mobilities can be set to

$$(\nu_{LV}, \nu_{SV}, \nu_{SL}) = (1, 0^+, 0^+),$$

in order to fix the solid phase. This set of coefficients is harmonically additive in the sense that, with the convention $\frac{1}{0^+} = +\infty$, there exist three non negative coefficients ν_S, ν_L and ν_V such that

$$\nu_{LV}^{-1} = \nu_L^{-1} + \nu_V^{-1}, \quad \nu_{SV}^{-1} = \nu_S^{-1} + \nu_V^{-1} \text{ and } \quad \nu_{SL}^{-1} = \nu_S^{-1} + \nu_L^{-1}.$$

Indeed, we can just consider $\nu_S = 0^+$ and $\nu_L = \nu_V = 2$.

Having in mind the application to wetting, we assume in the rest of the paper that:

- the surface tensions are additive, i.e. there exist coefficients $\sigma_i \geq 0$, $i \in \{1, \dots, L\}$, such that $\sigma_{ij} = \sigma_i + \sigma_j$, $\forall i, j \in \{1, \dots, L\}$;
- the mobility coefficients are harmonically additive, i.e. there exist nonnegative coefficients ν_i satisfying $\nu_{ij}^{-1} = \nu_i^{-1} + \nu_j^{-1}$ (with the convention that $\frac{1}{0^+} = +\infty$).

With such assumptions, it is easy to reformulate the expression of the L-phase perimeter in the more convenient following form

$$P(\Omega_1, \dots, \Omega_L) = \sum_{i=1}^{L} \sigma_i P(\Omega_i), \tag{2}$$

which can be approximated in the sense of Γ-convergence by a sum of scalar Cahn-Hilliard energies defined for every smooth $\mathbf{u} = (u_1, \dots, u_L) \in \mathbb{R}^L$ by

$$P_\varepsilon(\mathbf{u}) = \begin{cases} \displaystyle\sum_{k=1}^{L} \sigma_k \int_\Omega \left(\frac{\varepsilon}{2} |\nabla u_k|^2 + \frac{1}{\epsilon} W(u_k) \right) dx & \text{if } \sum_{k=1}^{L} u_k = 1, \\ +\infty & \text{otherwise,} \end{cases}$$

In this definition each u_i represents a smooth approximation of the characteristic function $\mathbb{1}_{\Omega_i}$, $W(s) = \frac{s^2(1-s)^2}{2}$ is a double-well potential, and the parameter ε characterizes the width of the diffuse interface, i.e. how concentrated is each $\nabla u_i dx$ around the Hausdorff measure supported on the reduced boundary of Ω_i.

Since the multiphase surface diffusion flow is the H^{-1}-gradient flow of (2), a natural idea to approximate it is to consider the H^{-1}-gradient flow of P_ε which yields the following Cahn-Hilliard system

$$\begin{cases} \varepsilon^2 \partial_t u_k = \nu_k \Delta \left(\sigma_k \mu_k + \lambda \right) \\ \mu_k = W'(u_k) - \varepsilon^2 \Delta u_k, \end{cases}$$

where λ is the Lagrange multiplier associated with the partition constraint $\sum u_k = 1$. Here, we follow the idea of [**?**] to handle the set $\{\nu_{i,j}\}$ of mobilities and we use explicitly its harmonic additive decomposition.

However, the asymptotic expansion of this phase field system is not clear and to the best of our knowledge, no analysis of its convergence has been made so far. The main obstacle to overcome is the non local nature of the system, which is particularly significant in the multiphase case.

In [**?**], we reviewed various two-phase Cahn-Hilliard systems and we proposed a new one. It basically involves degenerate mobilities that vanish in pure phase regions, therefore localize the system and allow to prove asymptotic results. In the next paragraph we sum up the properties and choices of parameters in the biphasic case which we will extend to the multiphase case. We refer to [**?**] for details.

Recall that [**?**, **?**] proved that the classical Cahn-Hilliard equation

$$\begin{cases} \varepsilon^2 \partial_t u = \Delta \mu, \\ \mu = W'(u) - \varepsilon^2 \Delta u, \end{cases}$$

does not converge to surface diffusion flow but rather to the Hele-Shaw model which is non local. Cahn and al. [**?**] introduced a new system involving a concentration-dependent mobility M. It is often referred as a degenerate mobility in the sense that no motion occurs in the pure states regions. Cahn and al. proposed the following equation that we will refer to as **M-CH** :

$$\begin{cases} \varepsilon^2 \partial_t u = \operatorname{div} \left(M(u) \mu \right), \\ \mu = W'(u) - \varepsilon^2 \Delta u. \end{cases}$$

A formal convergence to the correct motion is shown in [**?**]. However, the particular model studied by Cahn et al invoves a logarithmic potential W, which raises numerical issues. Instead, the potential commonly chosen in the literature and the one that we will use for the remainder of this paper is the smooth potential

$$W(s) = \frac{1}{2} s^2 (1-s)^2.$$

The choice of the mobility M has been discussed theoretically in [**?**, **?**, **?**]. It is proven by a formal asymptotic method that the choice $M(u) = u(1-u)$ does not lead to the correct velocity as an additional bulk diffusion term appears. These conclusions have been corroborated numerically in [**?**, **?**] where undesired coarsening effects are observed. Actually a quartic mobility $M(u) = u^2(1-u)^2$ is necessary to recover the correct velocity. These conclusions have been extended to the anisotropic case in [**?**]. From now on, we fix

$$M(s) = s^2(1-s)^2.$$

While the **M-CH** model has the correct sharp interface limit and produces satisfactory numerical results, it has a well identified drawback. In the asymptotic, the leading error term is of order 1 and becomes relevant when reaching the pure states $0, 1$, causing oscillations and an imprecise profile for the solution. The problem is two-fold. Firstly, the solution does not remain within the physical range of $[0, 1]$, which means that in the multiphase context, some phases might not be positive in some areas (in other words, the so-called *positivity property* is not fulfilled). Secondly, this induces some numerical volume losses despite the natural volume

preservative nature of the Cahn-Hilliard equation as illustrated in [**?**].

In [**?**], the authors managed to improve the numerical accuracy by introducing another degeneracy in the model. It has been successfully adapted in various applications, see for example [**?**, **?**, **?**, **?**]. Despite its numerical property, the aforementioned model does not derive from an energy. It is thus more difficult to prove rigorously theoretical properties and to extend the model to complex multiphase applications. Therefore, a variational adaptation has been proposed in [**?**] where the second degeneracy is injected in the energy. Because it relies on modifying the energy, it makes it more complex to extend to complex multiphase applications or to add an anisotropy.

In [**?**], we proposed a different approach where an additional mobility N was incorporated in the metric of the gradient flow instead of plugging it into the energy, and thus the geometry of the evolution problem. The so-called **NMN-CH** model proposed in [**?**] reads as

$$\begin{cases} \varepsilon^2 \partial_t u &= N(u) \operatorname{div}\left(M(u) \nabla (N(u)\mu)\right) \\ \mu &= W'(u) - \varepsilon^2 \Delta u, \end{cases}$$

The presence of two supplementary terms $N(u)$ is needed to ensure the variational nature of the model. Using formal asymptotic expansion, we showed in [**?**] that the correct choice for N is

$$N(s) = \frac{1}{\sqrt{M(s)}} = \frac{1}{s(1-s)},$$

Indeed, it allows to nullify the error term of order 1 in the solution, making the **NMN-CH** model of order 2. The profile obtained for the solution u is very accurate and the volume conservation is ensured up to an error of order 2, to be compared with the order 1 for **M-CH**. As observed in [**?**], another choice for N which avoids issues with the pure phases $s = 0, 1$ without changing the conclusions of the asymptotic expansion is $N(s) = \frac{1}{\sqrt{s^2(1-s)^2 + \gamma \varepsilon^2}}$, with $\gamma > 0$.

Concerning the positivity property, it is not strictly fulfilled in the biphase case but almost, with a better numerical accuracy for the **NMN-CH** model in comparison with the **M-CH** model, see [**?**]. While there is still an overshoot of the solution that goes beyond the physical range when reaching the pure states, it is of order $\mathcal{O}(\varepsilon^2)$ for **NMN-CH** mode and $\mathcal{O}(\varepsilon)$ for **M-CH**.

In this paper, we extend the **M-CH** and **NMN-CH** models to the case of L phases. From the modeling viewpoint, this amounts to integrating in the model the influence of surface tensions σ_{ij} and phase mobilities ν_{ij}. To this end, we adapt to the Cahn-Hilliard system the work of [**?**] done for the Allen-Cahn system. In particular, we propose to analyze the two following phase field models, where in both cases λ is the Lagrangian multiplier which encodes the partition constraint $\sum_{k=1}^{L} u_k = 1$:

- The **M-CH** multiphase field model defined for $k \in \{1, \dots, L\}$ by:

$$\begin{cases} \varepsilon^2 \partial_t u_k = \nu_k \operatorname{div}\left(M(u_k) \nabla (\sigma_k \mu_k + \lambda)\right), \\ \mu_k = W'(u_k) - \varepsilon^2 \Delta u_k, \end{cases} \tag{3}$$

  with mobility $M(s) = 2W(s)$.
- The **NMN-CH** multiphase field model defined for $k \in \{1, \dots, L\}$ by:

$$\begin{cases} \varepsilon^2 \partial_t u_k = \nu_k N(u_k) \operatorname{div}\left(M(u_k) \nabla (\sigma_k N(u_k) \mu_k + \lambda)\right), \\ \mu_k = W'(u_k) - \varepsilon^2 \Delta u_k. \end{cases} \tag{4}$$

with mobilities $M(s) = 2W(s)$ and $N(s) = 1/\sqrt{M(s)}$. This model is well defined whenever $u \neq 0, 1$, which is the case near the interface $\{u = \frac{1}{2}\}$. To give sense to the model in the whole domain, it can be rewritten in two different ways:

- either by transferring N to the left-hand side to obtain the alternative model

(5) (**NMN-CH** reformulation I)
$$\begin{cases} \varepsilon^2 g(u_k)\partial_t u_k = \nu_k \operatorname{div}\left(M(u_k)\nabla(\sigma_k\mu_k + \lambda)\right), \\ g(u_k)\mu_k = W'(u_k) - \varepsilon^2\Delta u_k. \end{cases}$$

  where $g(u_k) = \sqrt{M(u_k)}$ is always well-defined. Such a reformulation (strictly equivalent where $M(u_k)$ does not vanish) will be used for the asymptotic expansion.
- or by modifying the definitions of M, N to prevent them from vanishing while preserving the conclusions of the asymptotic expansion. This is the case with the following model:

(**NMN-CH** reformulation II)
$$\begin{cases} \partial_t u_k &= \nu_k \tilde{N}(u_k) \operatorname{div}\left(\tilde{M}(u_k)\nabla\tilde{N}(u_k)(\sigma_k\mu_k + \lambda)\right) \\ \mu_k &= \frac{W'(u_k)}{\varepsilon^2} - \Delta u_k \end{cases}$$

where the mobilities $\tilde{M}$ and $\tilde{N}$ are defined by $\tilde{M}(s) = 2W(s)+\gamma\varepsilon^2$ and $\tilde{N}(s) = \frac{1}{\sqrt{\tilde{M}(s)}}$, with $\gamma > 0$. Obviously, $\tilde{M}$ never vanishes and $\tilde{N}$ is well-defined everywhere. We will explain in the first lines of Section 2.3 why this reformulation has the same asymptotic properties as the original model (4). The **NMN-CH** reformulation II model will be used for numerical approximation (because numerical errors require a choice for M that prevents cancellations).

1.1. **Outline of the paper.** We first proceed to a formal asymptotic analysis of the **M-CH** and **NMN-CH** multiphase models. In particular, we show that the limit law of each model is indeed the multiphase surface diffusion flow with the advantage that **NMN-CH** guarantees an approximation error of order 2 in ε. In a second section, devoted to numerical approximation, we first introduce a numerical scheme suitable for both models. This scheme is based on a Fourier-spectral convex-concave semi implicit approach in the spirit of [**?**, **?**]. We provide numerical experiments which illustrate the stability of our scheme and the asymptotic properties of both phase field models. In the last section, we consider the special case of the wetting / dewetting phenomenon for which we derive a simplified model using the liquid phase only. We illustrate this model with 3D numerical experiments using either smooth or rough surfaces, and choosing various set of parameters to get different Young angle conditions.

2. Formal matched asymptotic expansions

In this section, we give a formal proof of Propositions 2.1 and 2.2 below using the method of matched asymptotic expansions. These results involve the so-called *optimal profile* q associated with the potential W and defined by the equation $q'(z) = -\sqrt{2W(q(z))}$ with a suitable constraint on $q(0)$. In the case where $W(s) = \frac{1}{2}s^2(1-s)^2$ and $q(0) = \frac{1}{2}$, one gets

$$q(z) = \frac{1 - \tanh\left(\frac{z}{2}\right)}{2}.$$

The following constants are also used in both propositions:

$$c_W = \int_{\mathbb{R}} \left(q'(z)\right)^2 dz, \quad c_M = \int_{\mathbb{R}} M(q(z))dz \quad \text{and} \quad c_N = \int_{\mathbb{R}} \frac{q'(z)}{N(q(z))}dz.$$

Remark that with our particular choices for N and q, one has $c_N = -c_W$.

Proposition 2.1. *For $i, j \in \{1, \dots, L\}$ with $i \neq j$, let $\Omega_i^\varepsilon = \{x,\ u_i(x) \geq \frac{1}{2}\}$ and*

$$\Gamma_{ij}^\varepsilon = \partial\Omega_i^\varepsilon \cap \{x,\ u_j \geq u_k,\ k \in \{1, \dots, L\} \setminus \{i\}\}.$$

The solution $\mathbf{u}^\varepsilon$ to the **M-CH** *model defined for $k \in \{1, \dots, L\}$ by*

$$\begin{cases} \varepsilon^2\partial_t u_k = \nu_k \operatorname{div}\left(M(u_k)\nabla(\sigma_k\mu_k + \lambda)\right), \\ \mu_k = W'(u_k) - \varepsilon^2\Delta u_k, \end{cases}$$

satisfies (formally) near the interface Γ_{ij}^ε the following asymptotic expansions:

$$\begin{cases} u_i^\varepsilon = q\left(\dfrac{\mathrm{dist}(x,\Omega_i^\varepsilon)}{\varepsilon}\right) + \mathcal{O}(\varepsilon), \\ u_j^\varepsilon = 1 - q\left(\dfrac{\mathrm{dist}(x,\Omega_i^\varepsilon)}{\varepsilon}\right) + \mathcal{O}(\varepsilon), \\ u_k^\varepsilon = \mathcal{O}(\varepsilon). \end{cases}$$

where $\mathrm{dist}(\cdot,\Omega_i^\varepsilon)$ denotes the signed distance function to Ω_i^ε.
Moreover, the normal velocity V_{ij}^ε at the interface Γ_{ij}^ε satisfies (formally):

$$\frac{1}{\nu_{ij}} V_{ij}^\varepsilon = \sigma_{ij} c_M c_W \Delta_\Gamma H_{ij} + \mathcal{O}(\varepsilon).$$

Proposition 2.2. *With the notations of Proposition 2.1, the solution $\mathbf{u}^\varepsilon$ to the* **NMN-CH** *model defined for $k \in \{1,\dots,L\}$ by*

$$\begin{cases} \varepsilon^2 \partial_t u_k = \nu_k N(u_k)\,\mathrm{div}\left(M(u_k)\nabla(\sigma_k N(u_k)\mu_k + \lambda)\right), \\ \mu_k = W'(u_k) - \varepsilon^2 \Delta u_k, \end{cases}$$

satisfies (formally) near the interface Γ_{ij}^ε the following asymptotic expansions:

$$\begin{cases} u_i^\varepsilon = q\left(\dfrac{\mathrm{dist}(x,\Omega_i^\varepsilon)}{\varepsilon}\right) + \mathcal{O}(\varepsilon^2), \\ u_j^\varepsilon = 1 - q\left(\dfrac{\mathrm{dist}(x,\Omega_i^\varepsilon)}{\varepsilon}\right) + \mathcal{O}(\varepsilon^2), \\ u_k^\varepsilon = \mathcal{O}(\varepsilon^2). \end{cases}$$

Moreover, the normal velocity V_{ij}^ε at the interface Γ_{ij}^ε satisfies (formally):

$$\frac{1}{\nu_{ij}} V_{ij}^\varepsilon = \sigma_{ij} \frac{c_W c_M}{(c_N)^2} \Delta_\Gamma H_{ij} + \mathcal{O}(\varepsilon).$$

To prove these propositions, we first recall the tools necessary for our derivations following the notations of **[?, ?, ?]**. We follow closely the presentation of these tools in **[?]**. We first proceed to the asymptotic expansion for the **M-CH** model. The proof is shown in dimension 2 only for the sake of simplicity of notations and readability, but it can be readily extended to higher dimensions. We end up with the **NMN-CH** model, which we have to rewrite to avoid indeterminate forms. For the most part, the calculations remain the same as for the biphasic case presented in **[?]**.

2.1. **Formal asymptotic analysis toolbox.** In this multiphase context, we study the behavior of the system in two regions: near the interface $\Gamma := \Gamma_{ij}$ separating two given phases $i \neq j$, and far from it. We denote u_k the solution for an arbitrary phase k. Whether k can designate i or j in an equation will be clear from the context.

To derive the method we require that the interface $\Gamma = \Gamma_{ij}$ remains smooth enough so that there exist $\delta > 0$ and a neighborhood

$$\mathcal{N} = \mathcal{N}_{ij}^\delta(\Gamma) = \{x \in \Omega / |d(x,t)| < 3\delta\},$$

in which the signed distance function $d := d_{ij}$ to Γ is well-defined. $\mathcal{N}$ is called the *inner region* near the interface and its complement the *outer region*.

Outer variables:
Far from the interface, we consider the *outer functions* (u_k, μ_k) depending on the standard *outer variable* x. The systems remain the same, namely for **M-CH**:

$$\begin{cases} \varepsilon^2 \partial_t u_k = \nu_k\,\mathrm{div}(M(u_k)\nabla(\sigma_k\mu_k + \lambda)), \\ \mu_k = -\varepsilon^2 \Delta u_k + W'(u_k). \end{cases} \tag{6}$$

Inner variables:
Inside $\mathcal{N}$ we consider the *inner variables* (z, s) associated with the original variables (x, t) in the following way: $z = \frac{d(x,t)}{\varepsilon}$ is a variable along the normal direction to the interface Γ and $s = S(x, t)$ is associated with a parameterization $X_0(s, t)$ of Γ.We define the *inner functions* U, $\mathfrak{U}$ depending on (z, s) as follows:

$$\begin{cases} U(z,s,t) := U\left(\dfrac{d(x,t)}{\varepsilon}, S(x,t), t\right) = u(x,t) \\ \mathfrak{U}(z,s,t) := \mathfrak{U}\left(\dfrac{d(x,t)}{\varepsilon}, S(x,t), t\right) = \mu(x,t) \end{cases}$$

In order to express the derivatives U_k, we first need to calculate the gradient and the Laplacian of d and S. The properties of d are well-known, see for instance [**?**]:

$$\begin{cases} \nabla d(x,t) = n(x,t), \\ \Delta d(x,t) = \displaystyle\sum_{l=1}^{d-1} \frac{\kappa_l(\pi(x))}{1+\kappa_l(\pi(x))d(x,t)} = \frac{H}{1+\varepsilon z H} \text{ in dimension 2.} \end{cases}$$

where π is the orthogonal projection onto Γ and $\kappa_1, \ldots, \kappa_{d-1}$ are the principal curvatures on Γ.

Given a point $X_0(s, t)$ on Γ, let

$$X(z, s, t) = X_0(s, t) + \epsilon z n(s, t).$$

whose orthogonal projection onto Γ is $X_0(s, t)$. The equation connecting the variable s and the function S is:

$$s = S(X_0(s, t) + \varepsilon z n(s, t), t).$$

Deriving this equation with respect to z leads to

$$0 = \varepsilon n \cdot \nabla S = \varepsilon \nabla d \cdot \nabla S.$$

which implies there is no cross derivative term. The derivation of the same equation with respect to s gives

$$1 = (\partial_s X_0 + \varepsilon z H \partial_s n) \cdot \nabla S = (1 + \varepsilon z H)\tau \cdot \nabla S.$$

Since ∇S is orthogonal to n, therefore collinear with the tangent τ, we have that:

$$\nabla S = \frac{1}{1+\varepsilon z H}\tau$$

Taking the divergence, we find ΔS:

$$\begin{aligned} \Delta S &= \operatorname{div}\left(\frac{\tau}{1+\varepsilon z H}\right) = \nabla\left(\frac{1}{1+\varepsilon z H}\right)\cdot\tau + \frac{1}{1+\varepsilon z H}\operatorname{div}(\tau), \\ &= \frac{1}{1+\varepsilon z H}\partial_s\left(\frac{1}{1+\varepsilon z H}\right) + \frac{1}{1+\varepsilon z H}\tau\cdot\partial_s\tau, \\ &= -\frac{\varepsilon z \partial_s H}{(1+\varepsilon z H)^3}. \end{aligned}$$

To express the connection between the derivatives of U_k, $\mathfrak{U}_k$ and u_k, μ_k, we come back to the definition of the inner functions:

$$u_k(x,t) = U_k\left(\frac{d(x,t)}{\varepsilon}, S(x,t), t\right).$$

Successive derivations with respect to x give the following equations

$$\begin{cases} \nabla u_k = \nabla d \dfrac{1}{\varepsilon}\partial_z U_k + \nabla S \partial_s U_k, \\ \Delta u_k = \Delta d \dfrac{1}{\varepsilon}\partial_z U_k + \dfrac{1}{\varepsilon^2}\partial_{zz} U_k + \Delta S \partial_s U_k + |\nabla S|^2 \partial_{ss} U_k, \\ \operatorname{div}\left(M(u_k)\nabla(N(u_k)\mu_k)\right) = \dfrac{1}{\varepsilon^2}\left(\partial_z M_k \partial_z (N_k \boldsymbol{\mu}_k)\right) + \dfrac{M_k}{\varepsilon}\Delta d \partial_z (N_k \boldsymbol{\mu}_k), \\ \qquad\qquad + |\nabla S|^2 \partial_s \left(M_k \partial_s (N_k \boldsymbol{\mu}_k)\right) + \Delta S M_k \partial_s (N_k \boldsymbol{\mu}_k). \end{cases}$$

The *inner system* of the **M-CH** model near the interface Γ finally reads as:

$$\begin{cases} \dfrac{\varepsilon^2}{\nu_k}\left(\partial_t U_k + \partial_t S \partial_s U_k\right) - \dfrac{\varepsilon}{\nu_k} V_{ij} \partial_z U_k = \dfrac{1}{\varepsilon^2}\partial_z \left(M(U_k)\partial_z\left(\sigma_k \boldsymbol{\mu}_k + \Lambda\right)\right), \\ \qquad\qquad + \dfrac{M(U_k)}{\varepsilon}\partial_z\left(\sigma_k \boldsymbol{\mu}_k + \Lambda\right)\Delta d_{ij} + T_1(s), \\ \boldsymbol{\mu}_k = W'(U_k) - \partial_{zz} U_k + \varepsilon \Delta d_{ij} \partial_z U_k + \varepsilon^2 T_2(s), \\ \Delta d_{ij} = \dfrac{H_{ij}}{1 + \varepsilon z H_{ij}} = H_{ij} - \varepsilon z H_{ij}^2 + \mathcal{O}(\varepsilon^2), \\ T_1(s) = \dfrac{\partial_s (M(U_k)\partial_s(\sigma_k \boldsymbol{\mu}_k + \Lambda))}{(1+\varepsilon z H_{ij})^2} - \dfrac{M(U_k)\varepsilon z \partial_s H_{ij}}{(1+\varepsilon z H_{ij})^3}\partial_s(\sigma_k \boldsymbol{\mu}_k + \Lambda), \\ T_2(s) = \dfrac{1}{(1+\varepsilon z H)^2}\partial_{ss} U_k - \dfrac{\varepsilon z \partial_s H_{ij}}{(1+\varepsilon z H_{ij})^3}\partial_s U_k. \end{cases}$$

Note that the terms in T_1 and T_2 are high-order tangential terms that play a role only at the fourth order in the asymptotic expansion.

Independence in z of the normal velocity V_{ij}:
The normal velocity $V_{ij}(s,t)$ of the interface is defined by:

$$V_{ij}(s,t) = \partial_t X_0(s,t) \cdot n(s,t).$$

In the neighborhood $\mathcal{N}$, we have the following property (which is a direct consequence of the definition of the signed distance function):

$$d(X_0(s,t) + \varepsilon z n(s,t), t) = \varepsilon z.$$

Deriving this with respect to t yields:

$$V_{ij}(s,t) = \partial_t X_0(s,t) \cdot \nabla d(X_0(s,t) + \varepsilon z n(s,t), t) = -\partial_t d\left(X(z,s,t), t\right).$$

Thus, the function $\partial_t d(x,t)$ is independent of z and can be extended in the whole neighborhood by choosing

$$V_{ij}(X_0(s,t) + \varepsilon z n, t) := -\partial_t d(X_0(s,t) + \varepsilon z n, t) = V_{ij}(s,t).$$

This property of independence is crucial to be able to extract the velocity from integrals in z in the following derivations.

Taylor expansions:
We assume the following Taylor expansions for our functions:

$$
\begin{aligned}
u_k(x,t) &= u_k^{(0)}(x,t) + \varepsilon u_k^{(1)}(x,t) + \varepsilon^2 u_k^{(2)}(x,t) + \cdots \\
U_k(z,s,t) &= U_k^{(0)}(z,s,t) + \varepsilon U_k^{(1)}(z,s,t) + \varepsilon^2 U_k^{(2)}(z,s,t) + \cdots \\
\mu_k(x,t) &= \mu_k^{(0)}(x,t) + \varepsilon \mu_k^{(1)}(x,t) + \varepsilon^2 \mu_k^{(2)}(x,t) + \cdots \\
\boldsymbol{\mu}_k(z,s,t) &= \boldsymbol{\mu}_k^{(0)}(z,s,t) + \varepsilon \boldsymbol{\mu}_k^{(1)}(z,s,t) + \varepsilon^2 \boldsymbol{\mu}_k^{(2)}(z,s,t) + \cdots \\
\lambda_k(x,t) &= \varepsilon \lambda_k^{(1)}(x,t) + \varepsilon^2 \lambda_k^{(2)}(x,t) + \cdots \\
\Lambda_k(z,s,t) &= \varepsilon \Lambda_k^{(1)}(z,s,t) + \varepsilon^2 \Lambda_k^{(2)}(z,s,t) + \cdots
\end{aligned}
$$

Since the numbering of the phase is present as a subscript, we indicate the order in the Taylor expansion as a superscript in brackets. We can then compose these expansions with a regular function F:

$$
\begin{aligned}
F(U_k) = F(U_k^{(0)}) + \varepsilon F'(U_k^{(0)}) U_k^{(1)} + \varepsilon^2 \left[F'(U_k^{(0)}) U_k^{(2)} + \frac{F''(U_k^{(0)})}{2} (U_k^{(1)})^2 \right] \\
+ \varepsilon^3 \left[F'(U_k^{(0)}) U_k^{(3)} + F''(U_k^{(0)}) U_k^{(1)} U_k^{(2)} + \frac{F'''(U_k^{(0)})}{6} (U_k^{(1)})^3 \right] + \cdots
\end{aligned}
$$

To simplify the notations within the asymptotic expansion, we adopt the following notations for $M(u_k)$

$$
M(u_k) = m_k^{(0)} + \varepsilon m_k^{(1)} + \varepsilon^2 m_k^{(2)} + \cdots,
$$

where

$$
\begin{cases}
m_k^{(0)} = M(u_k^{(0)}), \\
m_k^{(1)} = M'(u_k^{(0)}) u_k^{(1)}, \\
m_k^{(2)} = M'(u_k^{(0)}) u_k^{(2)} + \dfrac{M''(u_k^{(0)})}{2} (u_k^{(1)})^2.
\end{cases}
$$

We adopt the same convention for any generic *outer function* $F(u_k)$ or *inner function* $F(U_k)$:

$$
\begin{aligned}
F(u_k) &= f_k^{(0)} + \varepsilon f_k^{(1)} + \varepsilon^2 f_k^{(2)} + \varepsilon^3 f_k^{(3)} + \cdots \\
F(U_k) &= F_k^{(0)} + \varepsilon F_k^{(1)} + \varepsilon^2 F_k^{(2)} + \varepsilon^3 F_k^{(3)} + \cdots
\end{aligned}
$$

Flux matching condition between inner and outer equations:
Instead of using the matching conditions directly between the first equations of the inner and outer systems, it is more convenient to do the matching for the flux

$$
j_k = M(u_k) \nabla(\sigma_k \mu_k + \lambda).
$$

j_k has the following Taylor expansion for the **M-CH** model

$$
\begin{aligned}
j_k = &\left[m_k^{(0)} \nabla(\sigma_k \mu_k^{(0)} + \lambda^{(0)}) \right] + \varepsilon \left[m_k^{(1)} \nabla(\sigma_k \mu_k^{(0)} + \lambda^{(0)}) + m_k^{(0)} \nabla(\sigma_k \mu_k^{(1)}) \lambda^{(1)}) \right] \\
&+ \varepsilon^2 \left[m_k^{(2)} \nabla(\sigma_k \mu_k^{(0)} + \lambda^{(0)}) + m_k^{(1)} \nabla(\sigma_k \mu_k^{(1)} + \lambda^{(1)}) + m_k^{(0)} \nabla(\sigma_k \mu_k^{(2)} + \lambda^{(2)}) \right] + \mathcal{O}(\varepsilon^3).
\end{aligned} \tag{7}
$$

In inner coordinates, we only need to express the normal part

$$
J_{k,n} := J_k \cdot n = \frac{M(U_k)}{\varepsilon} \partial_z (\sigma_k \boldsymbol{\mu}_k + \Lambda),
$$

as the tangential terms are of higher order. The normal part expands as

$$
\begin{aligned}
J_{k,n} = \; & \frac{1}{\varepsilon}\left[M_k^{(0)}\partial_z(\sigma_k\boldsymbol{\mu}_k^{(0)}+\Lambda^{(0)})\right], \\
& + \left[M_k^{(1)}\partial_z(\sigma_k\boldsymbol{\mu}_k^{(0)}+\Lambda^{(0)}) + M_k^{(0)}\partial_z(\sigma_k\boldsymbol{\mu}_k^{(1)}+\Lambda^{(1)})\right], \\
& + \varepsilon\left[M_k^{(2)}\partial_z(\sigma_k\boldsymbol{\mu}_k^{(0)}+\Lambda^{(0)}) + M_k^{(1)}\partial_z(\sigma_k\boldsymbol{\mu}_k^{(1)}+\Lambda^{(1)}) + M_k^{(0)}\partial_z(\sigma_k\boldsymbol{\mu}_k^{(2)}+\Lambda^{(2)})\right], \\
& + \varepsilon^2\Big[M_k^{(3)}\partial_z(\sigma_k\boldsymbol{\mu}_k^{(0)}+\Lambda^{(0)}) + M_k^{(2)}\partial_z(\sigma_k\boldsymbol{\mu}_k^{(1)}+\Lambda^{(1)}), \\
& \qquad + M_k^{(1)}\partial_z(\sigma_k\boldsymbol{\mu}_k^{(2)}+\Lambda^{(2)}) + M_k^{(0)}\partial_z(\sigma_k\boldsymbol{\mu}_k^{(3)}+\Lambda^{(3)})\Big] + \mathcal{O}(\varepsilon^3).
\end{aligned} \tag{8}
$$

The flux matching conditions allow to match the limit as $z \to \pm\infty$ of terms of (7) with the corresponding order terms of (8).

We can now investigate order by order the behavior of the **M-CH** model. We have to study up to the fourth order term where the leading order of the velocity will appear in the first equation of (6). After that, we adapt the argument to the **NMN-CH** model, where a reformulation of the problem will be necessary to avoid indeterminate forms in the asymptotic expansion.

2.2. **Formal matched asymptotic expansion for the multiphasic M-CH model.** We first establish Proposition 2.1 regarding the properties of the **M-CH** model. We recall that we study the behavior of the different terms of the system near the interface Γ_{ij} separating phases i and j. We assume the following matching conditions for the two phases:

$$
\begin{aligned}
&\lim_{z\to+\infty} U_i^{(0)} = 0, \quad \lim_{z\to-\infty} U_i^{(0)} = 1, \\
&\lim_{z\to+\infty} U_j^{(0)} = 1, \quad \lim_{z\to-\infty} U_j^{(0)} = 0.
\end{aligned}
$$

For the other phases, we require the following matching conditions

$$
\lim_{z\to\pm\infty} U_k^{(0)} = 0, \quad \lim_{z\to\pm\infty} U_k^{(1)} = 0.
$$

First order:
At order $(\mathcal{O}(\varepsilon^{-2}), \mathcal{O}(1))$ the inner system reads as

$$
\begin{cases}
0 = \partial_z\left(M_k^{(0)}\partial_z(\sigma_k\boldsymbol{\mu}_k^{(0)})\right), \\
\boldsymbol{\mu}_k^{(0)} = W'(U_k^{(0)}) - \partial_{zz}U_k^{(0)}.
\end{cases}
$$

From the first equation of the system, we deduce that $M_k^{(0)}\partial_z(\sigma_k\boldsymbol{\mu}_k^{(0)})$ is constant. The matching conditions for the outer flux (7) and the inner flux (8) at order ε^{-1} impose this constant to be zero. Then there is a constant $A_k^{(0)}$ such that

$$
\sigma_k\boldsymbol{\mu}_k^{(0)} = A_k^{(0)}.
$$

Collecting all this information, we obtain that:

$$
\partial_{zz}U_k^{(0)} - W'(U_k^{(0)}) = \frac{A_k^{(0)}}{\sigma_k} \quad \forall k \in \{1,\dots,L\}.
$$

We complement with the initial conditions

$$
\begin{cases}
U_i^{(0)} = U_j^{(0)} = \dfrac{1}{2} \\
U_k^{(0)} = 0 \quad \forall k \in \{1,\dots,L\}\setminus\{i,j\},
\end{cases}
$$

Finally, we conclude that

$$\begin{cases} U_i^{(0)} = q(z), \\ U_j^{(0)} = q(-z) = 1 - q(z), \\ U_k^{(0)} = 0 \quad \forall k \in \{1, \dots, L\} \setminus \{i, j\}, \\ \boldsymbol{\mu}_k^{(0)} = 0 \quad \forall k \in \{1, \dots, L\}, \end{cases}$$

where q is the optimal phase field profile.

Second order:
At order $(\mathcal{O}(\varepsilon^{-1}), \mathcal{O}(\varepsilon))$ the outer system reads as

$$\begin{cases} 0 = \partial_z \left(M_k^{(0)} \partial_z (\sigma_k \boldsymbol{\mu}_k^{(1)} + \Lambda^{(1)}) \right), \\ \boldsymbol{\mu}_k^{(1)} = W''(U_k^{(0)}) U_k^{(1)} - \partial_{zz} U_k^{(1)} - H_{ij} \partial_z U_k^{(0)}. \end{cases} \tag{9}$$

It follows that there exists a function $B_k^{(1)}$ constant in z such that

$$M_k^{(0)} \partial_z (\sigma_k \boldsymbol{\mu}_k^{(1)} + \Lambda^{(1)}) = B_k^{(1)}.$$

By the matching condition between the outer flux (7) and the inner flux (8) at order 1, it holds that

$$\lim_{z \to \pm\infty} M_k^{(0)} \partial_z (\sigma_k \boldsymbol{\mu}_k^{(1)} + \Lambda^{(1)}) = 0.$$

We deduce that $B_k^{(1)} = 0$ and that there exists a function $A_k^{(1)}$ constant in z such that

$$\sigma_k \boldsymbol{\mu}_k^{(1)} + \Lambda^{(1)} = A_k^{(1)}.$$

Subtracting the case $k = i$ from the case $k = j$ gives

$$\sigma_j \boldsymbol{\mu}_j^{(1)} - \sigma_i \boldsymbol{\mu}_i^{(1)} = A_j^{(1)} - A_i^{(1)}.$$

The term $A_{ij}^{(1)} := A_j^{(1)} - A_i^{(1)}$ can be determined using the second equation of (9). Indeed, recall that

$$\begin{cases} \sigma_i \boldsymbol{\mu}_i^{(1)} = \sigma_i W''(U_i^{(0)}) U_i^{(1)} - \sigma_i \partial_{zz} U_i^{(1)} - \sigma_i H_{ij} q', \\ \sigma_j \boldsymbol{\mu}_j^{(1)} = \sigma_j W''(U_k^{(0)}) U_j^{(1)} - \sigma_j \partial_{zz} U_j^{(1)} + \sigma_j H_{ij} q'. \end{cases}$$

We multiply both equations by q' and integrate the difference. We can eliminate the terms in $U^{(1)}$ through integration by parts:

$$\begin{aligned} \int_{\mathbb{R}} \partial_z (W'(U_i^{(0)}))(U_i^{(1)} - \partial_{zz} U_i^{(1)} \partial_z U_i^{(0)}) dz &= \left[W'(U_i^{(0)}) U_i^{(1)} - \partial_z U_i^{(1)} \partial_z U_i^{(0)} \right]_{-\infty}^{+\infty}, \\ &\quad - \int_{\mathbb{R}} \partial_z U_i^{(1)} \left(\underbrace{W'(U_i^{(0)}) - \partial_{zz} U_i^{(0)}}_{=0} \right) dz, \\ &= 0. \end{aligned}$$

It follows that

$$A_{ij}^{(1)} = -\int_{\mathbb{R}} (\sigma_j \boldsymbol{\mu}_j^{(1)} - \sigma_i \boldsymbol{\mu}_i^{(1)}) q' \, dz = -(\sigma_j + \sigma_i) H_{ij} \int_{\mathbb{R}} (q')^2 \, dz = -\sigma_{ij} c_W H_{ij}. \tag{10}$$

On the other hand, summing the second equation of system (9) for the phases i and j gives

$$\boldsymbol{\mu}_i^{(1)} + \boldsymbol{\mu}_j^{(1)} = W''(q) \left[U_i^{(1)} + U_j^{(1)} \right] - \partial_{zz} \left[U_i^{(1)} + U_j^{(1)} \right].$$

Multiplying by q' and integrating by parts gives:

$$\int_{\mathbb{R}} \left(\mu_i^{(1)} + \mu_j^{(1)}\right) q' dz = 0.$$

Thus there exists a profile ζ and a tangential function c such that

$$\mu_i^{(1)} + \mu_j^{(1)} = c(s)\zeta(z).$$

Combining this with equation (10), we obtain

$$\begin{cases} \mu_i^{(1)} = -c_W H_{ij} + \zeta(z)c(s)\dfrac{\sigma_i}{\sigma_{ij}}, \\ \mu_j^{(1)} = c_W H_{ij} + \zeta(z)c(s)\dfrac{\sigma_j}{\sigma_{ij}}. \end{cases}$$

and then,

$$\begin{cases} W''(U_i^{(0)})U_i^{(1)} - \partial_{zz}U_i^{(1)} = H_{ij}(c_W + q') + \zeta(z)c(s)\frac{\sigma_j}{\sigma_{ij}}, \\ W''(U_j^{(0)})U_j^{(1)} - \partial_{zz}U_j^{(1)} = -H_{ij}(c_W + q') + \zeta(z)c(s)\frac{\sigma_i}{\sigma_{ij}}. \end{cases}$$

which leads to

$$\begin{cases} U_i^{(1)}(z,s) = H_{ij}\eta(z) + c(s)\frac{\sigma_j}{\sigma_{ij}}\omega(z), \\ U_j^{(1)}(z,s) = -H_{ij}\eta(z) + c(s)\frac{\sigma_i}{\sigma_{ij}}\omega(z). \end{cases}$$

Here η and ω are two profiles defined as the solutions to $W'(q)y - y'' = q' + c_W$ and $W'(q)y - y'' = \xi$, respectively, with appropriate initial conditions.

In particular, if $H_{ij} \neq 0$, then $U_i^{(1)}$ and $U_j^{(1)}$ cannot vanish both together which explains why the leading error order term for the solution of the system is ε only. This yields the important conclusion that the **M-CH** model is *always of order* 1 when the mean curvature is non zero. It justifies the interest of the **NMN-CH** model which is of second order.

Third order:
At order $(\mathcal{O}(1), \mathcal{O}(\varepsilon^2))$ the inner system reads as

$$\begin{cases} 0 = \partial_z \left(M_k^{(0)} \partial_z (\sigma_k \mu_k^{(2)} + \Lambda^{(2)}) \right), \\ \mu_k^{(2)} = \dfrac{W'''(U_k^{(0)})}{2}(U_k^{(1)})^2 + W''(U_k^{(0)})U_k^{(2)} - \partial_{zz}U_k^{(2)} + H_{ij}\partial_z U_k^{(1)} - zH_{ij}^{(2)}\partial_z U_k^{(0)}. \end{cases} \tag{11}$$

In the first equation, we used the results from the first two orders and left out the term that vanishes. From the first equality of (11), we find that:

$$M_k^{(0)} \partial_z (\sigma_k \mu_k^{(2)} + \Lambda^{(2)}) = B_k^{(2)}.$$

The matching conditions between the flux (7) and (8) at order ε yields (by removing all the null terms):

$$B_k^{(2)} = \lim_{z \to \pm\infty} M_k^{(0)} \partial_z (\sigma_k \mu_k^{(2)} + \Lambda^{(2)}) = 0.$$

This means that the term $\sigma_k \mu_k^{(2)} + \Lambda^{(2)}$ is constant in z and will not intervene in the flux term of order ε^2.

Fourth order:
Collecting the previous results, the first equation of the inner system at order ε for the phase i

and j simplifies to

$$\begin{cases} -\dfrac{1}{\nu_i} V_{ij} q' = \partial_z \left[M_i^{(0)} \partial_z (\sigma_i \boldsymbol{\mu}_i^{(3)} + \Lambda^{(3)}) \right] + \partial_s \left[M_i^{(0)} \partial_s (\sigma_i \boldsymbol{\mu}_i^{(1)} + \Lambda^{(1)}) \right], \\ \dfrac{1}{\nu_j} V_{ij} q' = \partial_z \left[M_j^{(0)} \partial_z (\sigma_j \boldsymbol{\mu}_j^{(3)} + \Lambda^{(3)}) \right] + \partial_s \left[M_j^{(0)} \partial_s (\sigma_j \boldsymbol{\mu}_j^{(1)} + \Lambda^{(1)}) \right], \end{cases}$$

We subtract the two equations, and integrate. We divide the computation in three:

- The left hand side gives:

$$\left(\frac{1}{\nu_i} + \frac{1}{\nu_j} \right) V_{ij} = \frac{1}{\nu_{ij}} V_{ij}.$$

- Collecting the result from the previous paragraphs, we find the following matching between the outer flux (7) and the inner flux (8) at order ε^2:

$$\lim_{z \to \pm\infty} M_i^{(0)} \partial_z (\sigma_i \boldsymbol{\mu}_i^{(3)} + \Lambda^{(3)}) = m_i^{(1)} \nabla (\sigma_i \mu_i^{(1)} + \lambda^{(1)}).$$

  Because $M'(0) = M'(1) = 0$, the limit term is zero and then

$$\int_{\mathbb{R}} \partial_z \left(M_i^{(0)} \partial_z (\sigma_i \boldsymbol{\mu}_i^{(3)} + \Lambda^{(3)}) \right) dz = 0.$$

  The corresponding term for the j-th phase is treated similarly.

- Using (10), the second term of the right hand side is (noting that $M_i^{(0)} = M_j^{(0)}$):

$$\int_{\mathbb{R}} M_i^{(0)} \partial_{ss} (\sigma_i \boldsymbol{\mu}_i^{(1)} - \sigma_j \boldsymbol{\mu}_j^{(1)}) dz = \sigma_{ij} \left(\int_{\mathbb{R}} M(q(z)) dz \right) c_W \partial_{ss} H_{ij}.$$

Finally, we obtain that

$$\frac{1}{\nu_{ij}} V_{ij} = \sigma_{ij} c_W c_M \partial_{ss} H_{ij}.$$

2.3. **Formal matched asymptotic expansion for the multiphase NMN-CH model.** We now give a proof of Proposition 2.2 concerning the properties of **NMN-CH**. The following matching conditions for the phase i and j are assumed:

$$\lim_{z \to +\infty} U_i^{(0)} = 0, \quad \lim_{z \to -\infty} U_i^{(0)} = 1,$$
$$\lim_{z \to +\infty} U_i^{(0)} = 1, \quad \lim_{z \to -\infty} U_i^{(0)} = 0,$$

and for the other phases

$$\lim_{z \to \pm\infty} U_k^{(0)} = 0, \quad \lim_{z \to \pm\infty} U_k^{(1)} = 0.$$

Reformulation of the model:
It is more convenient to rewrite the **NMN-CH** model by transferring $N(u_k)$ to the left hand side of the system, which yields the **NMN-CH** reformulation I model we already mentioned:

$$\begin{cases} \varepsilon^2 g(u_k) \partial_t u_k = \nu_k \operatorname{div} \left(M(u_k) \nabla (\sigma_k \mu_k + \lambda) \right), \\ g(u_k) \mu_k = W'(u_k) - \varepsilon^2 \Delta u_k. \end{cases} \tag{12}$$

where $g(u_k) = \sqrt{M(u_k)} = \frac{1}{N(u_k)}$ when $N(u_k)$ is well-defined, and, as before, λ is the Lagrangian multiplier which encodes the partition constraint $\sum_{u_k} = 0$. As already said, the advantage of such a formulation is that $g(u_k)$ is always well defined even if $u_k = 0$, which is not the case for $N(u_k)$. Note also that the definition of μ_k has been changed but we keep the same notation for simplicity.

Remark that similar calculations as those shown below can be done for the **NMN-CH** reformulation II model which is used for numerical approximation, and the same conclusions of Proposition 2.2 hold. Actually, using the additional term $\gamma \varepsilon^2$ in the definition of M does not

change the asymptotic results for at least the first four orders of interests. Indeed, this term appears to be associated with $\boldsymbol{\mu}_0$ (see below) which is zero, and $\boldsymbol{\mu}_1$ whose derivative in z vanishes.

The inner system for **NMN-CH** reformulation I now reads (for simplicity, we drop the expression "reformulation I" in the calculations below):

$$\begin{cases} \dfrac{\varepsilon^2 G_k}{\nu_k}\partial_t U_k + \dfrac{\varepsilon^2 G_k}{\nu_k}\partial_t S \partial_s U_k - \dfrac{\varepsilon G_k}{\nu_k} V_{ij}\partial_z U_k = \dfrac{1}{\varepsilon^2}\partial_z\left(M_k \partial_z(\sigma_k \boldsymbol{\mu}_k + \Lambda)\right) \\ \qquad\qquad + \dfrac{M_k}{\varepsilon}\Delta d_{ij}\partial_z(\sigma_k\boldsymbol{\mu}_k + \Lambda) + T_1(s), \\ G_k \boldsymbol{\mu}_k = W'(U_k) - \partial_{zz}U_k - \varepsilon \Delta d_{ij}\partial_z U_k + \varepsilon^2 T_2(s), \\ \Delta d_{ij} = \dfrac{H_{ij}}{1+\varepsilon z H_{ij}} = H_{ij} - \varepsilon z H_{ij}^2 + \mathcal{O}(\varepsilon^2), \\ T_1(s) = \dfrac{1}{(1+\varepsilon z H_{ij})^2}\partial_s(M_k\partial_s(\sigma_k\boldsymbol{\mu}_k + \Lambda)) - \dfrac{\varepsilon z M_k \partial_s H_{ij}}{(1+\varepsilon z H_{ij})^3}\partial_s(\sigma_k\boldsymbol{\mu}_k + \Lambda), \\ T_2(s) = \dfrac{1}{(1+\varepsilon z H_{ij})^2}\partial_{ss}U_k - \dfrac{\varepsilon z \partial_s H_{ij}}{(1+\varepsilon z H_{ij})^3}\partial_s U_k. \end{cases}$$

Because the $N(u_k)$ are now on the left hand side of the system in the form of G_k, the flux term $j = M(u_k)\nabla(\sigma_k\mu_k + \lambda_k)$ is the same as the one for **M-CH**. The flux matching condition is then also equal to the one given by (7) and (8).

First order:
At order $(\mathcal{O}(\varepsilon^{-2}), \mathcal{O}(1))$ the inner system reads:

$$\begin{cases} 0 = \partial_z\left(M_k^{(0)}\partial_z(\sigma_k\boldsymbol{\mu}_k^{(0)})\right), \\ G_k^{(0)}\boldsymbol{\mu}_k^{(0)} = W'(U_k^{(0)}) - \partial_{zz}U_k^{(0)}. \end{cases}$$

From the first equation of the system, we deduce that $M_k^{(0)}\partial_z(\sigma_k\boldsymbol{\mu}_k^{(0)})$ is constant. The matching conditions on the outer (7) and inner fluxes (8) at order ε^{-1} impose this constant to be zero. Then there exists a constant $A_k^{(0)}$ in z such that

$$\sigma_k\boldsymbol{\mu}_k^{(0)} = A_k^{(0)}.$$

Collecting all this information, we have

$$\partial_{zz}U_k^{(0)} - W'(U_k^{(0)}) = \frac{G\left(U_k^{(0)}\right)A_k^{(0)}}{\sigma_k}, \quad \forall k \in \{1,\dots,L\}.$$

Then, using the matching conditions and the initial conditions $U_i^{(0)} = U_j^{(0)} = \frac{1}{2}$ leads to

$$\begin{cases} U_i^{(0)} = q(z), \\ \boldsymbol{\mu}_i^{(0)} = 0, \\ U_j^{(0)} = q(-z) = 1 - q(z), \\ \boldsymbol{\mu}_j^{(0)} = 0, \\ U_k^{(0)} = 0 \quad \forall k \in \{1,\dots,L\}\setminus\{i,j\}. \end{cases}$$

Notice that $\boldsymbol{\mu}_k^{(0)}$ is a constant in z that can be nonzero.

Second order:
At order $(\mathcal{O}(\varepsilon^{-1}), \mathcal{O}(\varepsilon))$ the inner system reads

$$\begin{cases} 0 = \partial_z \left(M_k^{(0)} \partial_z (\sigma_k \boldsymbol{\mu}_k^{(1)} + \Lambda^{(1)}) \right), \\ G_k^{(0)} \boldsymbol{\mu}_k^{(1)} + G_k^{(1)} \boldsymbol{\mu}_k^{(0)} = W''(U_k^{(0)}) U_k^{(1)} - \partial_{zz} U_k^{(1)} - H_{ij} \partial_z U_k^{(0)}. \end{cases} \tag{13}$$

For $k \neq i, j$, using the fact that $U_k^{(0)} = 0$, the second equation can be rewritten as

$$0 = \left(1 - \boldsymbol{\mu}_k^{(0)}\right) U_k^{(1)} - \partial_{zz} U_k^{(1)}.$$

As the matching conditions show that $\lim_{z \pm \infty} U_k^{(1)} = 0$, it follows that $U_k^{(1)} = 0$.

Now turning to the i-th phase (resp j-th), there exists a function $B_i^{(1)}$ constant in z such that

$$M_i^{(0)} \partial_z (\sigma_i \boldsymbol{\mu}_i^{(1)} + \Lambda^{(1)}) = B_i^{(1)}.$$

From the matching condition between outer (7) and inner flux (8) at order 1, we deduce that

$$\lim_{z \to \pm \infty} M_i^{(0)} \partial_z (\sigma_i \boldsymbol{\mu}_i^{(1)} + \Lambda^{(1)}) = 0,$$

and $B_i^{(1)} = 0$ (resp $B_j^{(1)} = 0$). Then there exist functions $A_i^{(1)}, A_j^{(1)}$ constant in z such that

$$\begin{cases} \sigma_i \boldsymbol{\mu}_i^{(1)} + \Lambda^{(1)} = A_i^{(1)}, \\ \sigma_j \boldsymbol{\mu}_j^{(1)} + \Lambda^{(1)} = A_j^{(1)}. \end{cases}$$

Subtracting the i-th term to the j-th term leads to

$$\sigma_j \boldsymbol{\mu}_j^{(1)} - \sigma_i \boldsymbol{\mu}_i^{(1)} = A_j^{(1)} - A_i^{(1)} := A_{ij}^{(1)}.$$

Moreover, recall that $U_k^{(1)} = 0$ for $k \neq i, j$, which implies that $U_i^{(1)} = -U_j^{(1)}$ as $\sum_{k=1}^N U_k^{(1)} = 0$. Using the symmetry properties $g(1-s) = g(s)$ and $W''(1-s) = W''(s)$, it follows that:

$$\begin{aligned} g(U_j^{(0)}) \boldsymbol{\mu}_j^{(1)} &= W''(U_j^{(0)}) U_j^{(1)} - \partial_{zz} U_j^{(1)} - H_{ij} \partial_z U_j^{(0)}, \\ &= -W''(U_i^{(0)}) U_i^{(1)} + \partial_{zz} U_i^{(1)} + H_{ij} \partial_z U_i^{(0)}, \\ &= -g(U_i^{(0)}) \boldsymbol{\mu}_i^{(1)}, \\ &= -g(U_j^{(0)}) \boldsymbol{\mu}_i^{(1)}. \end{aligned}$$

thus $g(U_j^{(0)}) \left(\boldsymbol{\mu}_i^{(1)} + \boldsymbol{\mu}_j^{(1)} \right) = 0$. Finally, as $g(q) \neq 0$, $\boldsymbol{\mu}_i^{(1)}$ and $\boldsymbol{\mu}_j^{(1)}$ are necessarily constant in z and

$$\boldsymbol{\mu}_j^{(1)} = -\boldsymbol{\mu}_i^{(1)}.$$

It shows that we can express $A_{ij}^{(1)}$ as

$$A_{ij}^{(1)} = (\sigma_j + \sigma_i) \boldsymbol{\mu}_j^{(1)} = -\sigma_{ij} \boldsymbol{\mu}_i^{(1)}.$$

Now, multiplying the second equation of (13) for phase i

$$g(U_i^{(0)}) \boldsymbol{\mu}_i^{(1)} = W''(U_i^{(0)}) U_i^{(1)} - \partial_{zz} U_i^{(1)} - H_{ij} q',$$

by the profile q' and integrating over $\mathbb{R}$ shows that

$$\boldsymbol{\mu}_i^{(1)} = -\frac{c_W}{c_N} H_{ij} \quad \text{and} \quad A_{ij}^{(1)} = \frac{c_W}{c_N} \sigma_{ij} H_{ij}. \tag{14}$$

Indeed, on the one hand we have

$$\begin{aligned}\int_{\mathbb{R}}(\partial_z(W'(U_i^{(0)}))U_i^{(1)}-\partial_{zz}U_i^{(1)}\partial_z U_i^{(0)})dz &= \left[W'(U_i^{(0)})U_i^{(1)}-\partial_z U_i^{(1)}\partial_z U_i^{(0)}\right]_{-\infty}^{+\infty},\\ &\quad -\int_{\mathbb{R}}\partial_z U_i^{(1)}\left(\underbrace{W'(U_i^{(0)})-\partial_{zz}U_i^{(0)}}_{=0}\right)dz,\\ &= 0,\end{aligned}$$

and on the other hand

$$\int_{\mathbb{R}} g(q)\boldsymbol{\mu}_i^{(1)}q'dz = \boldsymbol{\mu}_i^{(1)}\int_{\mathbb{R}}\frac{q'}{N(q)}dz = c_N\boldsymbol{\mu}_i^{(1)}, \quad \text{and} \int_{\mathbb{R}} H_{ij}(q')^2dz = c_W H_{ij}.$$

Finally, it shows that

$$\partial_{zz}U_i^{(1)}-W''(q)U_i^{(1)} = -H_{i,j}(q'-\frac{c_W}{c_N}g(q)).$$

Now, recall that the choice $M(s)=\sqrt{2W(s)}$ and $N(s)=1/\sqrt{M(s)}=1/\sqrt{2W(s)}$ for the mobilities implies that

$$g(q)=1/N(q)=\sqrt{2W(q)}=-q' \text{ and } c_N=-c_W.$$

This is the key point to understand why in this case the term $U_i^{(1)}$ is null as a solution of

$$\partial_{zz}U_i^{(1)}-W''(q)U_i^{(1)}=0.$$

The same argument gives $U_j^{(1)}=0$. In summary, we have $U_k^{(1)}=U_i^{(1)}=U_j^{(1)}=0$. It means that the leading error order term in the solutions U_i and U_j is of magnitude ε^2 while the other phases are absent.
Third order:
At order $(\mathcal{O}(1),\mathcal{O}(\varepsilon^2))$, using both previous orders, the inner system simplifies to

$$\begin{cases}0=\partial_z\left(M_k^{(0)}\partial_z(\sigma_k\boldsymbol{\mu}_k^{(2)}+\Lambda^{(2)})\right),\\ G_k^{(0)}\boldsymbol{\mu}_k^{(2)}=\dfrac{W'''(U_k^{(0)})}{2}(U_k^{(1)})^2+W''(U_k^{(0)})U_k^{(2)}-\partial_{zz}U_k^{(2)}+H_{ij}\partial_z U_k^{(1)}-zH_{ij}^2\partial_z U_k^{(2)}.\end{cases}$$

From the first equality, we find that

$$M_k^{(0)}\partial_z(\sigma_k\boldsymbol{\mu}_k^2+\Lambda^2)=B_2.$$

The matching conditions at order ε for the fluxes given by (7) and (8) yield also (by removing all the null terms):

$$B_2=\lim_{z\to\pm\infty}M_k^{(0)}\partial_z(\sigma_k\boldsymbol{\mu}_k^{(2)}+\Lambda^{(2)})=0.$$

Therefore, $\sigma_k\boldsymbol{\mu}_k^{(2)}+\Lambda^{(2)}$ is constant in z and will not intervene in the flux term of order ε^2.

Remark 2.3. *It is possible to show that $U_i^{(2)}$ and $U_j^{(2)}$ are of the form*

$$U_j^{(2)}=-U_i^{(2)}=H_{ij}^2\zeta(z),$$

where ζ is the profile defined by

$$\begin{cases}y''(z)-W''(q)y(z)=zq'\\ y(0)=0\end{cases}$$

and which decreases to zero at infinity.

Fourth order:
Eliminating all the vanishing terms, the first equations for the i-th and j-th phase of the inner system read

(15)

$$-\frac{1}{\nu_i}V_{ij}g(U_i^{(0)})\partial_z U_i^{(0)} = \partial_z\left[M_i^{(0)}\partial_z\left(\sigma_i\boldsymbol{\mu}_i^{(3)}+\Lambda^{(3)}\right)\right]dz + \partial_s\left[M(U_i^{(0)})\partial_s\left(\sigma_i\boldsymbol{\mu}_i^{(1)}+\Lambda^{(1)}\right)\right]dz,$$
$$-\frac{1}{\nu_j}V_{ij}g(U_j^{(0)})\partial_z U_j^{(0)} = \partial_z\left[M_j^{(0)}\partial_z\left(\sigma_j\boldsymbol{\mu}_j^{(3)}+\Lambda^{(3)}\right)\right]dz + \partial_s\left[M(U_j^{(0)})\partial_s\left(\sigma_j\boldsymbol{\mu}_j^{(1)}+\Lambda^{(1)}\right)\right]dz.$$

Integrating over $\mathbb{R}$ yields to

$$-\frac{c_N}{\nu_i}V_{ij} = \int_{\mathbb{R}}\partial_z\left[M(U_i^{(0)})\partial_z\left(\sigma_i\boldsymbol{\mu}_i^{(3)}+\Lambda^{(3)}\right)\right]dz + \int_{\mathbb{R}}\partial_s\left[M(U_i^{(0)})q'\partial_s\left(\sigma_i\boldsymbol{\mu}_i^{(1)}+\Lambda^{(1)}\right)\right]dz,$$
$$+\frac{c_N}{\nu_j}V_{ij} = \int_{\mathbb{R}}\partial_z\left[M(U_j^{(0)})\partial_z\left(\sigma_j\boldsymbol{\mu}_j^{(3)}+\Lambda^{(3)}\right)\right]dz + \int_{\mathbb{R}}\partial_s\left[M(U_j^{(0)})q'\partial_s\left(\sigma_j\boldsymbol{\mu}_j^{(1)}+\Lambda^{(1)}\right)\right]dz.$$

The matching conditions for the fluxes at order $\mathcal{O}(\varepsilon^2)$ show that the first integral is zero. Note that most of the terms in the fluxes have been proven to be zero in the previous orders.

On the other hand, the second integral can be expressed with the terms from the second order calculations and the properties of the profile q give that

$$\begin{aligned}\int_{\mathbb{R}}\partial_s\left[M(U_i^{(0)})\partial_s\left(\sigma_i\boldsymbol{\mu}_i^{(1)}+\Lambda^{(1)}\right)\right]dz &= \partial_{ss}\left(\sigma_i\boldsymbol{\mu}_i^{(1)}+\Lambda^{(1)}\right)\int_{\mathbb{R}}M(q)dz,\\ &= c_M\partial_{ss}\left(\sigma_i\boldsymbol{\mu}_i^{(1)}+\Lambda^{(1)}\right).\end{aligned}$$

The same result can be obtained for the integral in j. Subtracting the first equation of (15) to the second, we get

$$\frac{1}{\nu_{ij}}c_N V_{ij} = \left(\frac{1}{\nu_i}+\frac{1}{\nu_j}\right)c_N V_{ij} = c_M\partial_{ss}\left(-\sigma_i^{(1)}\boldsymbol{\mu}_i^{(1)}-\Lambda^{(1)}+\sigma_j\boldsymbol{\mu}_j^{(1)}+\Lambda^{(1)}\right) = c_M\partial_{ss}A_{ij}^{(1)}.$$

Using (14), it follows that

$$\frac{1}{\nu_{ij}}V_{ij} = \frac{c_W c_M}{(c_N)^2}\sigma_{ij}\partial_{ss}H_{ij},$$

which concludes the proof of Proposition 2.2.

3. Numerical approximation

In this section, we show how to compute efficiently numerical approximations to the solutions to phase field models **M-CH** and **NMN-CH** , and we provide various numerical illustrations of the performances and properties of both models in dimensions 2 and 3. The numerical approximation is performed with the original **M-CH** model and with the **NMN-CH** reformulation II model (see the introduction), whose definitions are recalled:

- **M-CH**

$$\begin{cases}\partial_t u_k &= \nu_k\,\mathrm{div}\left(M(u_k)\nabla(\sigma_k\mu_k+\lambda)\right)\\ \mu_k &= \frac{W'(u_k)}{\varepsilon^2}-\Delta u_k\\ 1 &= \sum_k u_k\end{cases}$$

  where the mobility M is defined as $M(u) = \frac{1}{c_N^2}2W(u)$. Here, the constant $|c_N| = \frac{1}{6}$ is added to get the same limit law as with our new Cahn–Hilliard model.
- **NMN-CH**-reformulation II

$$\begin{cases}\partial_t u_k &= \nu_k N(u_k)\,\mathrm{div}\left(M(u_k)\nabla N(u_k)(\sigma_k\mu_k+\lambda)\right)\\ \mu_k &= \frac{W'(u_k)}{\varepsilon^2}-\Delta u_k\\ 1 &= \sum_k u_k\end{cases}$$

where the mobilities M, N are defined by $M(s) = 2W(s)+\gamma\varepsilon^2$, with $\gamma > 0$, and $N(s) = \frac{1}{\sqrt{M(s)}}$. For simplicity we keep the original notations M, N although the definitions are different, and still for the sake of simplicity we drop the expression "reformulation II". We set $\gamma = 1$ for all numerical experiments presented below.

Various schemes have already been proposed in the literature, see [**?**, **?**, **?**, **?**], to deal with multiphase Cahn-Hilliard type equations, especially when the number of phases is $L = 3$ [**?**, **?**, **?**, **?**, **?**, **?**, **?**] or $L = 4$ [**?**, **?**, **?**, **?**].

Recall that the Cahn-Hilliard system is of fourth-order in space, which introduces severe restrictions on the time step for most classical methods due to numerical instability. To overcome these difficulties, a natural idea is to adapt the strategy of convex splitting of the Cahn–Hilliard energy which was first proposed by Eyre [**?**]. This technique has become very popular for it provides simple, efficient, and stable schemes to approximate various evolution problems with a gradient flow structure [**?**, **?**, **?**, **?**, **?**, **?**, **?**]. For instance, a first- and second-order splitting scheme was proposed in [**?**, **?**, **?**] to address the case of the Cahn–Hilliard equation with mobility. However, these approaches are based on finite elements and require the resolution of linear systems at each step, which can be ill-conditioned in the case of degenerate mobilities. As an alternative, we proposed recently in [**?**] a semi-implicit Fourier spectral method in the spirit of [**?**, **?**, **?**, **?**, **?**]. The idea is to exploit the variational structure of the mobility by using an additionally convex splitting of the associated metric. It gives a very simple, efficient, and stable scheme even in the case of degenerate mobilities.

An accurate non linear multigrid method was proposed in [**?**] to approximate the solution to the Cahn-Hilliard equation. However, this approach requires the resolution of a $2L \times 2L$ system of equations which can be problematic when L is large. Based on the first-order convex splitting method, Lee and al [**?**] developed a practically unconditionally gradient-stable conservative nonlinear numerical scheme for converting the L-phase Cahn–Hilliard system into a system of L Cahn–Hilliard equations. This reduces significantly the computational cost. More recently, Yang and Kim [**?**] proposed an unconditionally stable with second-order accuracy based on the Crank-Nicolson scheme and adopted the idea of stabilized method [**?**].

In this paper, we propose to adapt to multiphase the approach we proposed in [**?**]. The novelty is to split the treatment of the Lagrange multiplier via the splitting of the metric so that **M-CH** and **NMN-CH** can be solved in a decoupled way. This means that we only need to solve L biphasic Cahn–Hilliard equations at each iteration, as in [**?**].

In the following, we first recall the schemes we have introduced in [**?**] when only two phases (i.e. one single u) are considered for both **M-CH** and **NMN-CH** models. Then we extend to the multiphase case by using a semi-implicit treatment of the Lagrange multiplier which is explicitly given in Fourier space. For each model, a **Matlab** script is provided to give an example of implementation. Next, we provide a numerical comparison of phase field models in space dimension 2. In addition, some illustrations are provided to show the influence of mobilities and surface tensions using the **NMN-CH** model. These illustrations show also that our models can handle Cahn–Hilliard problems in complex domain without imposing any boundary condition or additional surface energy, but rather by simply imposing a null mobility at the appropriate interfaces. Then we conclude the section with an application to the wetting problem where we derive a simplified model using the liquid phase only.

3.1. **Spatial and time discretization: a Fourier-spectral approach.** All equations are solved on a square-box $Q = [0, L_1] \times \cdots \times [0, L_d]$ with periodic boundary conditions. We recall that the Fourier $\boldsymbol{K}$-approximation of a function u defined in a box $Q = [0, L_1] \times \cdots \times [0, L_d]$ is given

by

$$u^{\boldsymbol{K}}(x) = \sum_{\boldsymbol{k}\in K_N} c_{\boldsymbol{k}} e^{2i\pi \boldsymbol{\xi}_k \cdot x},$$

where $K_N = [-\frac{N_1}{2}, \frac{N_1}{2} - 1] \times [-\frac{N_2}{2}, \frac{N_2}{2} - 1] \cdots \times [-\frac{N_d}{2}, \frac{N_d}{2} - 1]$, $\boldsymbol{k} = (k_1, \ldots, k_d)$ and $\boldsymbol{\xi}_k = (k_1/L_1, \ldots, k_d/L_d)$. In this formula, the $c_{\boldsymbol{k}}$'s denote the K^d first discrete Fourier coefficients of u. The inverse discrete Fourier transform leads to $u^K_{\boldsymbol{k}} = \text{IFFT}[c_{\boldsymbol{k}}]$ where $u^K_{\boldsymbol{k}}$ denotes the value of u at the points $x_{\boldsymbol{k}} = (k_1 h_1, \ldots, k_d h_d)$ and where $h_i = L_i/N_i$ for $i \in \{1, \ldots, d\}$. Conversely, $c_{\boldsymbol{k}}$ can be computed as the discrete Fourier transform of $u^K_{\boldsymbol{k}}$, *i.e.*, $c_{\boldsymbol{k}} = \text{FFT}[u^K_{\boldsymbol{k}}]$.

Given a time discretization parameter $\delta_t > 0$, we construct a sequence $(u^n)_{n\geq 0}$ of approximations of u at times $n\delta_t$.

3.2. **Numerical scheme for the M-CH model.** We first recall the numerical approach introduced in [**?**] to compute numerical solutions of the **M-CH** model in a biphasic context. In such a case, the Cahn–Hilliard equation reads as

$$\begin{cases} \partial_t u &= \operatorname{div}\left(M(u)\nabla(\mu)\right), \\ \mu &= \frac{W'(u)}{\varepsilon^2} - \Delta u. \end{cases}$$

Our approach can be viewed as a Fourier semi-implicit scheme which reads as

$$\begin{cases} (u^{n+1} - u^n)/\delta_t &= m\Delta\mu^{n+1} + \operatorname{div}((M(u^n) - m)\nabla\mu^n) \\ \mu^{n+1} &= \left(-\Delta u^{n+1} + \frac{\alpha}{\varepsilon^2} u^{n+1}\right) + \left(\frac{1}{\varepsilon^2}(W'(u^n) - \alpha u^n)\right). \end{cases}$$

where m and α are two stabilization parameters. More precisely, this scheme derives from a convex-concave splitting of the Cahn–Hilliard energy

$$\int_Q (\frac{|\nabla u|^2}{2} + \frac{1}{\varepsilon^2} W(u))dx = \frac{1}{2}\int_Q (|\nabla u|^2 + \frac{\alpha}{\varepsilon^2}u^2)dx + \int_Q \frac{1}{\varepsilon^2}(W(u) - \alpha\frac{u^2}{2})dx,$$

but also of the associated metric

$$\frac{1}{2}\int_Q M(u^n)|\nabla\mu|^2 dx = \frac{1}{2}\int_Q m|\nabla\mu|^2 dx + \frac{1}{2}\int (M(u^n) - m)|\nabla\mu|^2 dx.$$

As we explained in [**?**], the scheme seems to decrease the Cahn–Hilliard energy as soon as each explicit term is concave, which is true when setting $m = \max_{s\in[0,1]} M(s)$ and $\alpha \geq \max_{s\in[0,1]} |W''(s)|$.

Alternatively this scheme reads in a matrix form as

$$\begin{pmatrix} I_d & -\delta_t m\Delta \\ \Delta - \alpha/\varepsilon^2 & I_d \end{pmatrix} \begin{pmatrix} u^{n+1} \\ \mu^{n+1} \end{pmatrix} = \begin{pmatrix} B^1_{u^n,\mu^n} \\ B^2_{u^n,\mu^n} \end{pmatrix},$$

where

$$\begin{pmatrix} B^1_{u^n,\mu^n} \\ B^2_{u^n,\mu^n} \end{pmatrix} = \begin{pmatrix} u^n + \delta_t \operatorname{div}((M(u^n) - m)\nabla\mu^n) \\ \frac{1}{\varepsilon^2}(W'(u^n) - \alpha u^n) \end{pmatrix}.$$

Finally, the couple (u^{n+1}, μ^{n+1}) can be computed using the system

$$\begin{cases} u^{n+1} &= L_M\left[B^1_{u^n,\mu^n} + \delta_t m\Delta B^2_{u^n,\mu^n}\right], \\ \mu^{n+1} &= L_M\left[(-\Delta B^1_{u^n,\mu^n} + \alpha/\varepsilon^2 B^1_{u^n,\mu^n}) + B^2_{u^n,\mu^n}\right], \end{cases}$$

where the operator

$$L_M = \left(I_d + \delta_t m\Delta(\Delta - \alpha/\varepsilon^2 I_d)\right)^{-1},$$

can be computed very efficiently in Fourier space.

Remark 3.1. *This scheme is very efficient as it does not require any resolution of a linear system. Moreover, this scheme seems to be stable without assumption on δ_t in the sense that it decreases the Cahn-Hilliard energy. It is also not difficult to show that the mass of u is conserved along the iterations, i.e.,*

$$\int_Q u^{n+1} dx = \int_Q u^n dx.$$

Following this method, we now propose similar schemes for the multiphase **M-CH** model

$$\begin{cases} \partial_t u_k & = \nu_k \operatorname{div}\left(M(u_k)\nabla(\sigma_k \mu_k + \lambda)\right), \\ \mu_k & = \frac{W'(u_k)}{\varepsilon^2} - \Delta u_k, \\ 1 & = \sum_k u_k. \end{cases}$$

They are based on the same convex-concave splitting of the Cahn-Hilliard equation and its associated metric. In the multiphase context, we obtain

$$\begin{cases} (u_k^{n+1} - u_k^n)/\delta_t & = \nu_k \left(m\Delta \left[\sigma_k \mu_k^{n+1} + \lambda^{n+1}\right] + \operatorname{div}\left[(M(u_k^n) - m)\nabla\left[\sigma_k \mu_k^n + \lambda^n\right]\right]\right), \\ \mu_k^{n+1} & = \left(-\Delta u_k^{n+1} + \frac{\alpha}{\varepsilon^2} u_k^{n+1}\right) + \left(\frac{1}{\varepsilon^2}(W'(u_k^n) - \alpha u_k^n)\right), \end{cases}$$

where the Lagrange multiplier λ^{n+1} is associated to the partition constraint $\sum_k u_k^{n+1} = 1$.

More precisely, the couple (u_k^{n+1}, μ_k^{n+1}) can be expressed as

$$\begin{cases} u_k^{n+1} & = u_k^{n+1/2} + \delta_t \nu_k m L_{M_k}\left[\Delta \lambda^{n+1}\right], \\ \mu_k^{n+1} & = \mu_k^{n+1/2} + \delta_t \nu_k m L_{M_k}\left[(-\Delta + \frac{\alpha}{\varepsilon^2})\Delta \lambda^{n+1}\right], \end{cases}$$

where

- the operator L_{M_k} is given by

$$L_{M_k} = \left(I_d + \delta_t m \sigma_k \nu_k \Delta(\Delta - \alpha/\varepsilon^2 I_d)\right)^{-1}.$$

- the couple $(u_k^{n+1/2}, \mu_k^{n+1/2})$ is defined as the solution to the decoupled system

$$\begin{cases} u_k^{n+1/2} & = L_{M_k}\left[B^1_{u_k^n, \mu_k^n} + \delta_t m \sigma_k \nu_k \Delta B^2_{u_k^n, \mu_k^n}\right], \\ \mu_k^{n+1/2} & = L_{M_k}\left[(-\Delta + \alpha/\varepsilon^2) B^1_{u_k^n, \mu_k^n} + B^2_{u_k^n, \mu_k^n}\right], \end{cases}$$

  where

$$B^1_{u_k^n, \mu_k^n} = u_k^n + \delta_t \nu_k \operatorname{div}\left[(M(u_k^n) - m)\nabla\left[\sigma_k \mu_k^n + \lambda^k\right]\right],$$

  and

$$B^2_{u_k^n, \mu_k^n} = \frac{1}{\varepsilon^2}(W'(u_k^n) - \alpha u_k^n).$$

In particular, λ^{n+1} satisfies the equation

$$\delta_t m \left(\sum_k \nu_k L_{M_k}\right) \Delta \lambda^{n+1} = 1 - \sum_k u_k^{n+1/2},$$

therefore,

$$\lambda^{n+1} = \frac{1}{\delta_t m}\left[\sum_k \nu_k L_{M_k} \Delta\right]^{-1} (1 - \sum_k u_k^{n+1/2}).$$

Here the operator $[\sum_k \nu_k L_{M_k}\Delta]^{-1}$ is still homogeneous and can be computed easily in Fourier space.

From the previous equations, we can implement the schemes within the **Matlab** framework almost immediately, see the 54-lines **Matlab** script of Table 1 which approximates the solution to the **M-CH** model. In particular :

- We consider here a discretized computation box $Q = [-1/2, 1/2]^2$ using $N = 2^8$ nodes in each direction. The initial condition of u is a uniform noise and the numerical parameters are set to $\varepsilon = 1/N$, $\delta_t = \varepsilon^4$, $\alpha = 2$, and $m = \max_{s\in[0,1]} M(s)$.
- First we define the terms $u_k^{n+1/2}$ and $\mu_k^{n+1/2}$ (lines 29-39) as in [**?**]. Then, we determine λ^{n+1} (lines 42-45) which allows us to correct and obtain u_k^{n+1} and μ_k^{n+1} (lines 48-52).
- Line 24 corresponds to the definition of the Fourier-symbol associated with the operator L_{M_k}. The application of L_{M_k} can then be performed by using a simple multiplication in Fourier space with the array M_L.
- Each computation of a gradient or a divergence is made in Fourier space. For instance the divergence $\operatorname{div}\left[(M(u_k^n) - m)\nabla\left[\sigma_k\mu_k^n + \lambda^k\right]\right]$ is computed on line 31.
- The computation of λ^{n+1} is illustrated on lines 42-45. λ^{n+1} is first computed in Fourier space using the Fourier-symbol of the operator $[\sum_k \nu_k L_{M_k}\Delta]^{-1}$. Then λ^{n+1} is obtained by applying the discrete inverse Fourier transform.

3.3. **Numerical scheme for the NMN-CH model.** The case of the **NMN-CH** model is slightly more complicated. We first recall the numerical scheme introduced in [**?**] for only two phases, then we explain how to generalize it in the multiphase context. Recall that the **NMN-CH** model reads in the biphase case as

$$\begin{cases} \partial_t u &= N(u)\operatorname{div}\left(M(u)\nabla(N(u)\mu)\right) \\ \mu &= \frac{W'(u)}{\varepsilon^2} - \Delta u \end{cases}$$

and that the Fourier semi-implicit scheme we proposed in [**?**] to approximate its solutions is

$$\begin{cases} (u^{n+1} - u^n)/\delta_t &= [m\Delta - \beta]\mu^{n+1} + H(u^n, \mu^n), \\ \mu^{n+1} &= \left(-\Delta u^{n+1} + \frac{\alpha}{\varepsilon^2}u^{n+1}\right) + \left(\frac{1}{\varepsilon^2}(W'(u^n) - \alpha u^n)\right), \end{cases}$$

where

$$H(u^n, \mu^n) = N(u^n)\operatorname{div}((M(u^n)\nabla(N(u^n)\mu^n)) - m\Delta\mu^n + \beta\mu^n.$$

Remark 3.2. *Recall that this approach is based on the convex-concave splitting of the associated metric*

$$\frac{1}{2}\int_Q M(u)\left|\nabla(N(u)\mu)\right|^2 dx = J_{u,c}(\mu) + J_{u,e}(\mu),$$

with

$$J_{u,c}(\mu) = \frac{1}{2}\int_Q m|\nabla\mu|^2 dx + \frac{1}{2}\int_Q \beta\mu^2 dx$$

and

$$J_{u,e}(\mu) = \int_Q G(u)\cdot\nabla\mu\mu dx + \frac{1}{2}\int_Q (|G(u)|^2 - \beta)\mu^2 dx + \frac{1}{2}\int_Q (1-m)|\nabla\mu|^2 dx.$$

Here, $G(u) = -\frac{1}{2}\nabla(\log(M(u)))$, and as it is bounded is $H^1(Q)$, a sufficiently large choice for m and β should ensure the concavity of $J_{u,e}(\mu)$ and the stability of the scheme. In practice, we take $m = 1$ and $\beta = 1/\varepsilon^2$ for our numerical experiments and these values did not show any sign of instability regardless of the choice of the time step δ_t.

Finally, the couple (u^{n+1}, μ^{n+1}) is solution of the system

$$\begin{pmatrix} I_d & -\delta_t(m\Delta - \beta I_d) \\ \Delta - \alpha/\varepsilon^2 & I_d \end{pmatrix}\begin{pmatrix} u^{n+1} \\ \mu^{n+1} \end{pmatrix} = \begin{pmatrix} B^1_{u^n,\mu^n} \\ B^2_{u^n,\mu^n} \end{pmatrix},$$

with

$$\begin{pmatrix} B^1_{u^n,\mu^n} \\ B^2_{u^n,\mu^n} \end{pmatrix} = \begin{pmatrix} u^n + \delta_t H(u^n, \mu^n) \\ \frac{1}{\varepsilon^2}(W'(u^n) - \alpha u^n), \end{pmatrix},$$

```
clear all; colormap('jet');

 %%%%%%%%%%%%%%%%% parameters %%%%%%%%%%%%%%%%%%%%%%%%
N = 2^8; epsilon =1/N; dt = epsilon^4; T = 10^(-4);
W_prim = @(U) (U.*(U-1).*(2*U-1));
MobMM = @(U) 2*36/2*((((U).*(1-U)).^2) );
alpha = 2;x = linspace(0,1,N); c=max(MobMM(x));
%%%%%%%%%%%%%%%% condition initiale %%%%%%%%%%%%%%%
U(:,:,1) = 2*rand(N,N)/3; U(:,:,2) = rand(N,N).*(1 -U(:,:,1) );
U(:,:,3) = 1-(U(:,:,1) + U(:,:,2) );
Mu = 0*U;lambda = 0; lambda_fourier = 0;Mu_fourier = zeros(N,N,3);
for k=1:3, U_fourier(:,:,k) = fft2(U(:,:,k)); end

%%%%%%%%%%%%%%%%%%% coefficient - mobilite %%%%%%%%%%
sigma12 =1; sigma13 =1; sigma23 =1;
sigma(1) = (sigma12 + sigma13 - sigma23)/2;
sigma(2) = (sigma12 + sigma23 - sigma13)/2;
sigma(3) = (sigma23 + sigma13 - sigma12)/2;
mob(1) = 1; mob(2)= 1; mob(3) = 1;
%%%%%%%%%%%%%%%% Diffusion Fourier %%%%%%%%%%%%%%%%
k = [0:N/2,-N/2+1:-1];
[K1,K2] = meshgrid(k,k);
Delta = -4*pi^2*((K1.^2 + (K2).^2));
for k=1:3, M_L(:,:,k) = 1./(1 + dt*sigma(k)*mob(k)*(c*Delta).*(Delta - alpha/epsilon^2)); end
%%%%%%%%%%%%%%%%%%%%%%%%%%%%%%%%%%%%%%%%%%%%%%%%%%%%
k=1;
for i=1:T/dt,
%%%%%%%%%%%% computation of u^{n+1/2}_k, \mu^{n+1/2}_k
for k=1:3,
mobUk = MobMM(U(:,:,k));
div_mob_laplacien_fourier = 2*1i*pi*K1.*fft2((mobUk-c).*ifft2(2*1i*pi*K1.*(sigma(k)*Mu_fourier(:,:,k) +
     lambda_fourier)))...
   + 2*1i*pi*K2.*fft2((mobUk-c).*ifft2(2*1i*pi*K2.*(sigma(k)*Mu_fourier(:,:,k) + lambda_fourier)));
B1 = U_fourier(:,:,k) + dt*mob(k)*div_mob_laplacien_fourier;
B2 = fft2(W_prim(U(:,:,k))/epsilon^2 - alpha/epsilon^2*U(:,:,k));
U_fourier(:,:,k) = M_L(:,:,k).*(B1 + dt*mob(k)*sigma(k)*c*Delta.*B2);
U(:,:,k) = real(ifft2(U_fourier(:,:,k)));
Mu_fourier(:,:,k) = M_L(:,:,k).*((alpha/epsilon^2 - Delta).*B1 + B2);
Mu(:,:,k) = ifft2(Mu_fourier(:,:,k));
end

%%%%%%%%%%%%%%%%%%% computation of lambda and correction %%%%%%%%%%
Err_sum = fft2(1 - sum(U,3));
lambda_fourier = (1./((c*(M_L(:,:,1)*mob(1) +M_L(:,:,2)*mob(2) + M_L(:,:,3)*mob(3))).*Delta)).*Err_sum/dt;
lambda_fourier(1,1) = 0;
lambda = real(ifft2(lambda_fourier));

for k=1:3,
term = dt*(mob(k)*(c*Delta.*lambda_fourier));
U_fourier(:,:,k) = U_fourier(:,:,k) + M_L(:,:,k).*term;
Mu_fourier(:,:,k) = Mu_fourier(:,:,k) - (Delta - alpha/epsilon^2).*M_L(:,:,k).*term;
U(:,:,k) = real(ifft2(U_fourier(:,:,k)));
Mu(:,:,k) = ifft2(Mu_fourier(:,:,k));
end
end
```

TABLE 1. **Matlab** implementation of our scheme to approximate in dimension 2 the solutions to the **M-CH** model.

and satisfies

$$\begin{cases} u^{n+1} &= L_{NMN}\left[B^1_{u^n,\mu^n} + \delta_t(m\Delta B^2_{u^n,\mu^n} - \beta B^2_{u^n,\mu^n})\right] \\ \mu^{n+1} &= L_{NMN}\left[(-\Delta B^1_{u^n,\mu^n} + \alpha/\varepsilon^2 B^1_{u^n,\mu^n}) + B^2_{u^n,\mu^n}\right]. \end{cases}$$

where the operator $L_{NMN} = \left(I_d + \delta_t(m\Delta - \beta I_d)(\Delta - \alpha/\varepsilon^2 I_d)\right)^{-1}$ can be computed very efficiently in Fourier space.

We now propose to extend this approach to the multiphase case:

$$\begin{cases} \partial_t u_k &= \nu_k N(u_k)\,\mathrm{div}\left[M(u_k)\nabla[N(u_k)\sigma_k\mu_k + \lambda)]\right], \\ \mu_k &= \frac{W'(u_k)}{\varepsilon^2} - \Delta u_k, \\ 1 &= \sum_k u_k. \end{cases}$$

The scheme reads

$$\begin{cases} (u_k^{n+1} - u_k^n)/\delta_t &= \nu_k[m\Delta - \beta](\sigma_k\mu_k^{n+1} + \lambda^{n+1}) + H_k(u_k^n, \mu_k^n, \lambda^n) \\ \mu_k^{n+1} &= \left(-\Delta u_k^{n+1} + \frac{\alpha}{\varepsilon^2}u_k^{n+1}\right) + \left(\frac{1}{\varepsilon^2}(W'(u_k^n) - \alpha u_k^n)\right), \end{cases}$$

where

$$H_k(u_k^n, \mu_k^n, \lambda^n) = \nu_k\left(N(u_k^n)\,\mathrm{div}((M(u_k^n)\nabla(N(u_k^n)(\sigma_k\mu_k^n + \lambda^n))) - [m\Delta - \beta](\sigma_k\mu_k^n + \lambda^n)\right).$$

and λ^{n+1} is associated to the partition constraint $\sum_k u_k^{n+1} = 1$.

Let us now introduce the couple $(u_k^{n+1/2}, \mu_k^{n+1/2})$ defined by

$$\begin{cases} u_k^{n+1/2} &= L_{NMN,k}\left[B^1_{u_k^n,\mu_k^n,\lambda^n} + \delta_t\nu_k\sigma_k([m\Delta - \beta]B^2_{u_k^n,\mu_k^n,\lambda^n})\right] \\ \mu_k^{n+1/2} &= L_{NMN,k}\left[(-\Delta B^1_{u_k^n,\mu_k^n,\lambda^n} + \alpha/\varepsilon^2 B^1_{u_k^n,\mu_k^n,\lambda^n}) + B^2_{u_k^n,\mu_k^n,\lambda_k^n}\right]. \end{cases}$$

where

$$L_{NMN,k} = \left(I_d + \delta_t\nu_k\sigma_k(m\Delta - \beta I_d)(\Delta - \alpha/\varepsilon^2 I_d)\right)^{-1}$$

and

$$B^1_{u^n,\mu^n,\lambda^n} = u^n + \delta_t H(u^n, \mu^n, \lambda^n) \text{ and } \quad B^2_{u^n,\mu^n,\lambda^n} = \frac{1}{\varepsilon^2}(W'(u^n) - \alpha u^n).$$

It is not difficult to see that

$$\begin{cases} u_k^{n+1} &= u_k^{n+1/2} + \delta_t\nu_k L_{NMN,k}\left[[m\Delta - \beta]\lambda^{n+1}\right] \\ \mu_k^{n+1} &= \mu_k^{n+1/2} + \delta_t\nu_k L_{NMN,k}\left[(-\Delta + \frac{\alpha}{\varepsilon^2})(m\Delta - \beta)\lambda^{n+1}\right] \end{cases}$$

which shows that λ^{n+1} satisfies

$$\lambda^{n+1} = \frac{1}{\delta_t}\left[\sum_k \nu_k L_{NMN,k}(m\Delta - \beta)\right]^{-1}(1 - \sum_k u_k^{n+1/2}).$$

where the operator $[\sum_k \nu_k L_{NMN,k}(m\Delta - \beta)]^{-1}$ is homogeneous and can be, again, computed easily in Fourier space.

Similarly to the **M-CH** model, the implementation of the previous scheme is simple and efficient. We present in Table 2 an example of a **Matlab** script with less than 60 lines which implements the scheme approximating the solutions to the **NMN-CH** model. In particular :

- We consider here a computation box $Q = [-1/2, 1/2]^2$ discretized with $N = 2^8$ nodes in each direction. The initial condition of u is a uniform noise and the numerical parameters are set to $\varepsilon = 1/N$, $\delta_t = \varepsilon^4$, $\alpha = 2$, $\beta = 2/\varepsilon^2$ and $m = 1$.
- The implementation is almost identical to the previous model. Only the treatment of the divergence term $H_k(u_k^n, \mu_k^n, \lambda^n)$ makes a difference. The computation is done in lines 33 to 36 and is based on the following equality:

$$\begin{aligned} N(u)\,\mathrm{div}(M(u)\nabla(N(u)\mu)) &= \sqrt{M(u)}\Delta\left(N(u)\mu\right) + N(u)\nabla(M(u))\cdot\nabla(N(u)\mu) \\ &= \sqrt{M(u)}\Delta\left(N(u)\mu\right) + 2\nabla\left[\sqrt{M(u)}\right]\cdot\nabla(N(u)\mu), \end{aligned}$$

  as $N(u) = 1/\sqrt{M(u)}$, see **[?]** for more details.
- Figure 1 shows the function $u_2^n + 2u_3^n$ computed at different times t^n using this script.

We believe that the proposed implementation shows the simplicity, efficiency, and stability of our numerical scheme.

```
clear all;
%%%%%%%%%%%%%%%%% parameters %%%%%%%%%%%%%%%%%%%%%%%%
N = 2^8; epsilon =1/N; dt = epsilon^4; T = 10^(-4);
alpha = 2;gamma=1; beta = 2/epsilon^2;
W_prim = @(U) (U.*(U-1).*(2*U-1));
MobM = @(U) 1/2*((((U).*(1-U)).^2+epsilon^2) );
MobN = @(U) 1./sqrt(MobM(U) );
%%%%%%%%%%%%%%%%% initial condition %%%%%%%%%%%%%%%
U(:,:,1) = 2*rand(N,N)/3; U(:,:,2) = rand(N,N).*(1 -U(:,:,1) );
U(:,:,3) = 1-(U(:,:,1) + U(:,:,2) );
Mu = 0*U;lambda = 0; lambda_fourier = 0;Mu_fourier = zeros(N,N,3);
for k=1:3, U_fourier(:,:,k) = fft2(U(:,:,k)); end
%%%%%%%%%%%%%%%%%% surface tension coefficients - mobilities %%%%%%%%%%
sigma12 =1; sigma13 =1; sigma23 =1;
sigma(1) = (sigma12 + sigma13 - sigma23)/2;
sigma(2) = (sigma12 + sigma23 - sigma13)/2;
sigma(3) = (sigma23 + sigma13 - sigma12)/2;
mob(1) = 1; mob(2)= 1; mob(3) = 1;
%%%%%%%%%%%%%%%%% Kernel %%%%%%%%%%%%%%%%
k = [0:N/2,-N/2+1:-1]; [K1,K2] = meshgrid(k,k);
Delta = -4*pi^2*((K1.^2 + (K2).^2)); M_L = zeros(N,N,3);
for k=1:3,
M_L(:,:,k) = 1./(1 + dt*sigma(k)*mob(k)*(gamma*Delta - beta) .*(Delta - alpha/epsilon^2));
end
%%%%%%%%%%loop %%%%%%%%%%%%%%%%%%%
for i=1:T/dt,
%%%%%%%%%%%% computation of u^{n+1/2}_k, \mu^{n+1/2}_k
for k=1:3,
mobMUk = MobM(U(:,:,k)); mobNUk = MobN(U(:,:,k));
sqrtMk = sqrt(mobMUk); sqrtMk_fourier = fft2(sqrtMk);
nabla1_sqrtMk= real(ifft2(2*pi*1i*K1.*sqrtMk_fourier )); nabla2_sqrtMk= real(ifft2(2*pi*1i*K2.*
    sqrtMk_fourier ));
muN_fourier = fft2((sigma(k)*Mu(:,:,k) + lambda).*mobNUk);
nabla1_muN = real(ifft2(2*pi*1i*K1.*muN_fourier ));
nabla2_muN = real(ifft2(2*pi*1i*K2.*muN_fourier ));
laplacien_muN = real(ifft2(Delta.*muN_fourier ));
NdivMgradNMu = sqrtMk.*laplacien_muN + 2*(nabla1_sqrtMk.*nabla1_muN +nabla2_sqrtMk.*nabla2_muN);
B1 = U_fourier(:,:,k) + dt*(mob(k)*fft2(NdivMgradNMu) - mob(k)*(gamma*Delta-beta).*((sigma(k)*Mu_fourier
    (:,:,k)+lambda_fourier)));
B2 = fft2(W_prim(U(:,:,k))/epsilon^2 - alpha/epsilon^2*U(:,:,k));
U_fourier(:,:,k) = M_L(:,:,k).*(B1 + dt*mob(k)*sigma(k)*(gamma*Delta-beta).*B2);
U(:,:,k) = real(ifft2(U_fourier(:,:,k)));
Mu_fourier(:,:,k) = M_L(:,:,k).*((alpha/epsilon^2 - Delta).*B1 + B2);
Mu(:,:,k) = real(ifft2(Mu_fourier(:,:,k)));
end
%%%%%%%%%%%%%%%%%% computation of lambda and correction %%%%%%%%%%
Err_sum = fft2(1 - sum(U,3));
weight = (M_L(:,:,1)*mob(1) +M_L(:,:,2)*mob(2) + M_L(:,:,3)*mob(3)).*(gamma*Delta-1*beta);
lambda_fourier = (1./(weight)).*Err_sum/dt;
lambda = real(ifft2(lambda_fourier));
for k=1:3,
term = (mob(k)*M_L(:,:,k)./((M_L(:,:,1)*mob(1) +M_L(:,:,2)*mob(2) + M_L(:,:,3)*mob(3)))).*Err_sum;
U_fourier(:,:,k) = U_fourier(:,:,k) + term;
Mu_fourier(:,:,k) = Mu_fourier(:,:,k) - (Delta - alpha/epsilon^2).*term;
U(:,:,k) = real(ifft2(U_fourier(:,:,k)));
Mu(:,:,k) = real(ifft2(Mu_fourier(:,:,k)));
end
end
```

TABLE 2. **Matlab** implementation of our scheme to approximate in dimension 2 the solutions to the **NMN-CH** model.

3.4. **Numerical validation.**

3.4.1. *Asymptotic expansion and flow: a numerical comparison.* The first numerical example concerns the evolution of an initial connected set. For each Cahn–Hilliard model, we plot on Figure 2 the phase field function $u_2^n + 2u_3^n$ computed at different times t. Each experiment is

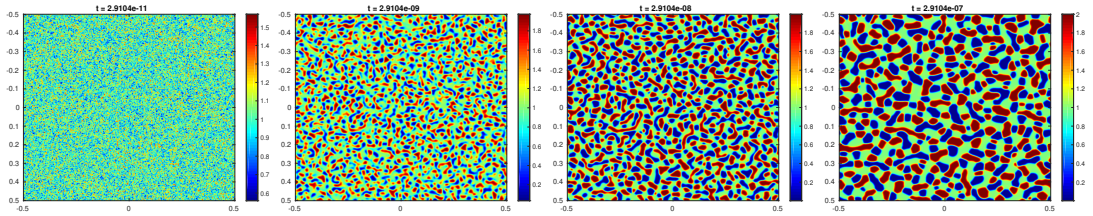

FIGURE 1. First numerical experiment using the **NMN-CH** model; the solutions u are computed with the **Matlab** script of Table 2. We plot the function $x \mapsto u_2(x) + 2u_3(x)$ on each picture which means that the first, second, and third phases appear in blue, green, and red, respectively.

performed using the same numerical parameters: $N = 2^8$, $\varepsilon = \delta_x$, $\delta_t = \varepsilon^4$, $\alpha = 2$, $m = 1$, and $\beta = 2/\varepsilon^2$.

The first and second lines of Figure 2 correspond to the solutions given by the **M-CH** and the **NMN-CH** models, respectively. Notice that the numerical experiments obtained with both models are very similar and should give a good approximation of the surface diffusion flow. In addition, for each model, the stationary flow limit appears to correspond to a ball of the same mass as that of the initial set.

To illustrate the asymptotic expansion performed in Section 2, we plot on Figure 3 (first two pictures) the slice $x_1 \mapsto u_1(x_1, 0)$ at the final time $T = 10^{-4}$. The profile associated to the **M-CH** model is plotted in red and clearly indicates that the solution u does not remain in the interval $[0, 1]$ with an overshoot of order $O(\varepsilon)$. In contrast, the profile obtained using the **NMN-CH** model (in green) seems to be very close to q and remains in $[0, 1]$ up to an error of order $O(\varepsilon^2)$. Finally, we plot the evolution of the Cahn–Hilliard energy along the flow for each model on the last picture of Figure 3. We can clearly observe a decrease of the energy in each case.

In conclusion, this first numerical experiment confirms the asymptotic expansion obtained in the previous section, and highlights the interest of our **NMN-CH** model to approximate surface diffusion flows.

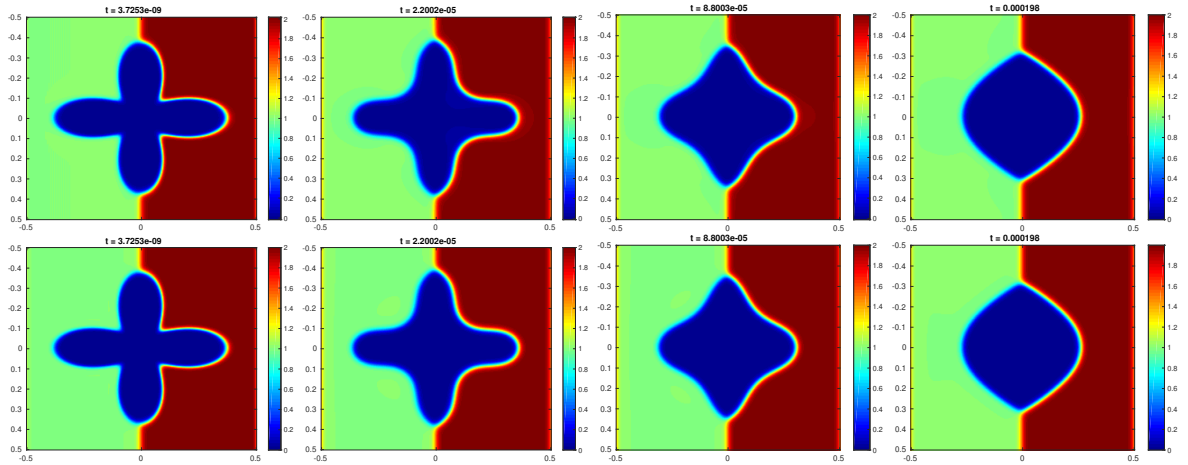

FIGURE 2. First numerical comparison of the two **CH** models: evolution of **u** along the iterations. First line using **M-CH**, second line using **NMN-CH**.

3.4.2. *Influence of the mobility using the* **NMN-CH** *model.* The second numerical experiment is intended to show the influence of surface mobilities (ν_{ij}) only on the velocity of each interface.

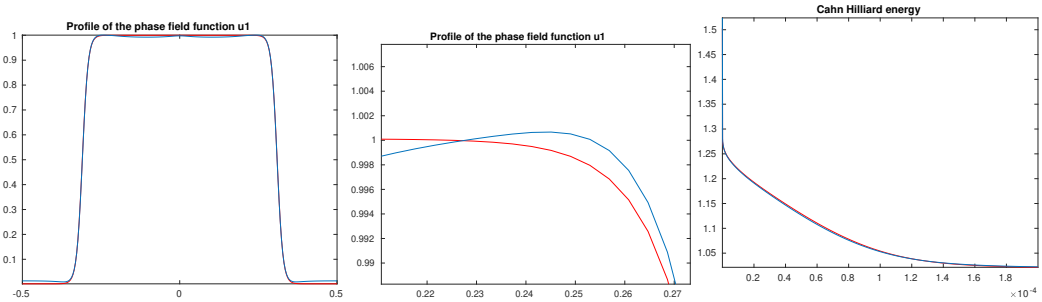

FIGURE 3. Comparison of the two different models: profile and energy; **M-CH** in blue, **NMN-CH** in red; First figure: slice of u: $x_1 \mapsto u_1(x_1, 0)$; Second figure: zoom on the slice of u_1; last figure: evolution of the Cahn–Hilliard energy along the flow.

To illustrate this, we show in Figure 4 the evolution of $\mathbf{u}$ in two different cases: a first case where $\nu_i = 1$ (see the first row on Figure 4); a second case where $\nu_2 = \nu_3 = 1$ and $\nu_1 = 0$ (see the second row). In both cases, the (σ_i) coefficients associated with surface tensions (σ_{ij}) are set to $\sigma_i = 1$. As previously, we use the same numerical parameters in each case: we set $N = 2^8$, $\varepsilon = 2/N$, $\delta_t = \varepsilon^4$, $\alpha = 2$, $m = 1$, and $\beta = 2/\varepsilon^2$.

As expected, we observe in the first row of Figure 4 that all phases are active along the iterations since the mobility coefficients ν_i are all equal to 1. On the contrary, in the second row, the first phase (u_1 in blue) is fixed along the iterations, which is consistent with the fact that the coefficient mobility associated with the first phase u_1 is $\nu_1 = 0$. Indeed, it is important to notice that mobilities play a role only in the gradient flow and therefore imposing a zero mobility $\nu_k = 0$ forces the k-th phase u_k to be fixed. In particular, this allows us to deal easily and efficiently with the Cahn–Hilliard problem in irregular domains (see [**?**, **?**, **?**, **?**, **?**]) and the second row of Figure 4 is a perfect illustration of it. We insist that our model does not impose any boundary conditions on the complex domain, nor the insertion of a surface energy. Another important remark is that the width of the diffuse interface depends only on ε and does not depend neither on surface tensions nor on mobilities.

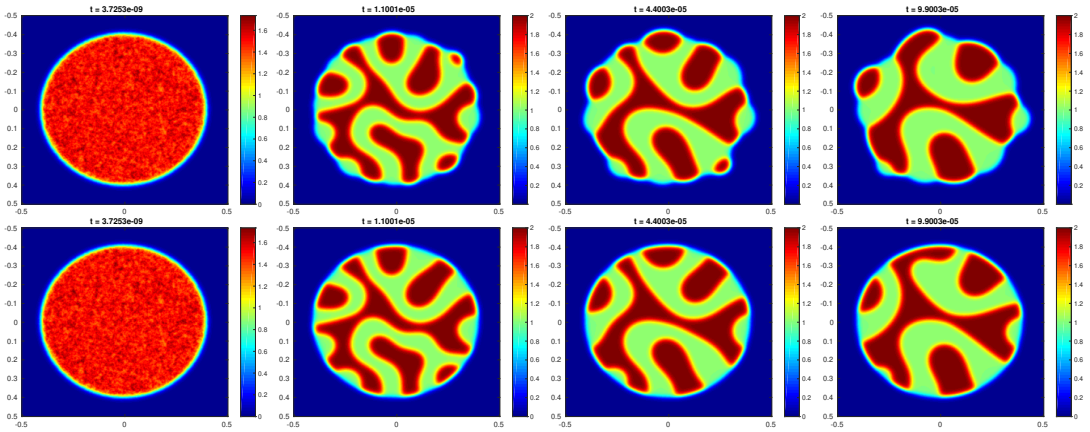

FIGURE 4. Influence of the mobility using **NMN-CH**: evolution of $\mathbf{u}$ along the iterations; First line using $\nu_1 = \nu_2 = \nu_3 = 1$; second line, using $\nu_1 = 0$ and $\nu_2 = \nu_3 = 1$.

3.4.3. *Influence of the surface tension coefficients using the* **NMN-CH** *model.* The **NMN-CH** model can also handle the case of the evolution of a liquid phase on a fixed solid surface by simply

imposing a null mobility of the solid interface. Here we propose an application in space dimension 2. Figure 5 illustrates numerical results obtained with different sets of surface tension coefficients $\sigma = (\sigma_{12}, \sigma_{13}, \sigma_{23})$, with mobilities $\nu_1 = 0,\ \nu_2 = \nu_3 = 1$ and the same initial condition: $\sigma = (1, 1, 1)$, $\sigma = (1.9, 1, 1)$ and $\sigma = (1, 1.9, 1)$ for the first, the second and the third rows of Figure 5, respectively. The solid u_1, liquid u_2 and vapor u_3 phases are represented in blue, red, and green, respectively. Similarly to the previous computations, the numerical parameters are set to $N = 2^8$, $\varepsilon = 2/N$, $\delta_t = \varepsilon^4$, $\alpha = 2$, $m = 1$, and $\beta = 2/\varepsilon^2$. As in the previous numerical experiment, we notice the ability of our model to handle the case of null mobilities (here to fix the exterior solid phase u_1 in blue). In Figure 5, we can also see the strong influence of the contact angle on the evolution of the liquid phase. We emphasize that our model does not prescribe the contact angle. Rather, its value is an implicit consequence of the multiphase interface energy considered in each simulation.

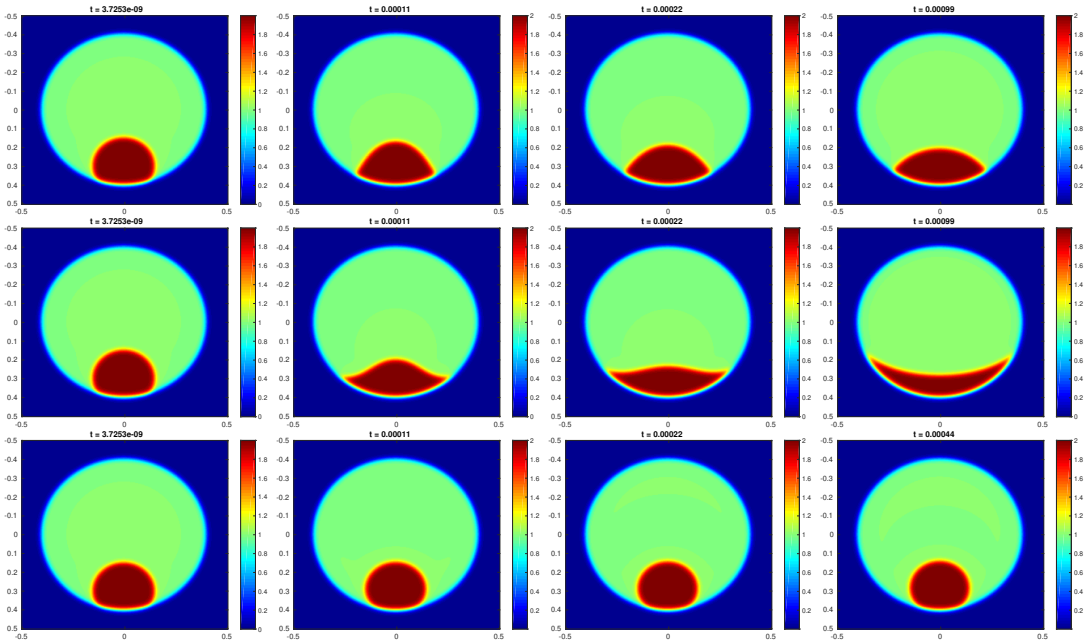

FIGURE 5. Influence of the surface tension coefficients using **NMN-CH**: evolution of $\mathbf{u}$ along the iterations; First line using $\sigma_{12} = \sigma_{13} = \sigma_{23} = 1$; second line using $\sigma_{12} = 1.9$ and $\sigma_{13} = \sigma_{23} = 1$; third line using $\sigma_{13} = 1.9$, and $\sigma_{12} = \sigma_{23} = 1$.

4. APPLICATION TO THE SIMULATION OF WETTING / DEWETTING

Let us recall that the behavior of liquids on solid surfaces has been of interest to the academic and engineering communities for many decades. Young [**?**] determined the optimal shape of a drop at equilibrium on a solid surface. More precisely, the shape of the drop minimizes the following energy:

$$P(\Omega_L) = \int_{\Gamma_{L,S}} \sigma_{L,S} \mathcal{H}^{d-1} + \int_{\Gamma_{L,V}} \sigma_{L,V} d\mathcal{H}^{d-1} + \int_{\Gamma_{L,V}} \sigma_{S,V} \mathcal{H}^{d-1},$$

under a constraint on the volume of the set Ω_L which represents the droplet. Here, $\sigma_{L,S}$, $\sigma_{L,V}$, and $\sigma_{L,V}$ are the surface tensions between the liquid (L), solid (S), and vapor (S) phases. In particular, the minimizers of this energy satisfy Young's law for the contact angle θ of the droplet with the solid.

$$\cos(\theta) = \frac{\sigma_{S,V} - \sigma_{S,L}}{\sigma_{L,V}}.$$

As illustrated in Figure 5, the approximation of such an evolution can be obtained using the previous phase field model with the following set of mobilities: $\nu_{LV} = 1$ and $\nu_{SV} = \nu_{SL} = 0$.

Other approaches have been developed, for example in [**?**] where Cahn proposed a phase-field approach to model the situation using an additional surface energy on the boundary of the solid phase. However, this method is only applicable for a contact angle $\theta < \frac{\pi}{2}$. An approach using the smoothed boundary conditions in order to force the correct contact angle condition is available in [**?**] within the Allen-Cahn equation context. Other methods relying on the Allen-Cahn equation using this idea are proposed in [**?**, **?**]. Alternative methods using wall boundary conditions with a third order polynomial to impose the contact angle have been proposed in [**?**, **?**, **?**]. A convexity splitting scheme using this idea with a sinusoidal boundary condition can be found in [**?**]. In [**?**, **?**, **?**, **?**, **?**] the angle is imposed using wall boundary conditions again. The dynamic case can be treated via a coupled Cahn–Hilliard/Navier-Stokes system. In most cases, see for example [**?**, **?**, **?**, **?**, **?**], the contact angle is set to the static contact angle $\frac{\pi}{2}$.

In the convolution-thresholding framework, some recent approaches have been proposed to simulate the wetting phenomenon. Expanding the original scheme of Bence, Merriman, and Osher [**?**], Esedoglu and Otto have proposed a multiphase convolution-thresholding method in [**?**] for arbitrary surface tensions satisfying the triangle inequality. Wang et al. then applied this generalization to the wetting case in [**?**]. A different approach proposed in [**?**] does not impose the contact angle in the formulation but requires the use of sophisticated techniques while solving the heat equation.

In [**?**, **?**], two of the authors proposed an Allen-Cahn equation where the solid phase was frozen in order to approximate droplet wetting. It was based on the use of zero surface mobilities for the solid-vapor and solid-liquid interfaces. In this paper, we extend this idea to the Cahn–Hilliard equation and, coupled with a reformulation of the problem, we introduce a new simple and efficient method for simulating the wetting phenomenon. It is important to emphasize that this method does not impose the contact angle, which is determined implicitly by the surface tension coefficients $(\sigma_{S,V}, \sigma_{S,L}, \sigma_{L,V})$.

4.1. **Rewriting of our phase field approach using the liquid phase only.** The motivation of this section is to present an equivalent phase field model using only one phase, the liquid phase, as Ω_S is fixed and Ω_V can be obtained from Ω_L and Ω_S. Indeed, numerical experiment in dimension 3 of a complete model (u_L, u_V, u_S) can be quite challenging numerically and it is preferable to reduce the system to the only unknown, the liquid phase.

Recall that in such a case, the Cahn-Hilliard energy reads as

$$P_\varepsilon(\mathbf{u}) = \sum_{k\in\{S,L,V\}} \frac{\sigma_k}{2} \int_Q \frac{\varepsilon}{2}|\nabla u_k|^2 + \frac{1}{\varepsilon} W(u_k),$$

where

$$\sigma_L = \frac{\sigma_{LS} + \sigma_{LV} - \sigma_{SV}}{2}, \sigma_S = \frac{\sigma_{LS} + \sigma_{SV} - \sigma_{LV}}{2} \text{ and } \sigma_V = \frac{\sigma_{LV} + \sigma_{SV} - \sigma_{LS}}{2}.$$

Here, u_S represents the phase field function associated with the solid set Ω_S and the previous asymptotic developments show that u_S should be of the form $u_S = q\left(\frac{\text{dist}(x,\Omega_S)}{\varepsilon}\right)$. On the other hand, the vapor phase field function u_V can be obtained using the partition constraint with $u_V = 1 - (u_S + u_L)$. Then the Cahn–Hilliard energy can be rewritten using only the variable

u_L as follows:

$$\begin{aligned}\tilde{P}_\varepsilon(u_L) &= \frac{\sigma_L}{2}\int_Q (\frac{\varepsilon}{2}|\nabla u_L|^2 + \frac{1}{\varepsilon}W(u_L))dx \\ &+ \frac{\sigma_V}{2}\int_Q (\frac{\varepsilon}{2}|\nabla(1-(u_S+u_L)|^2 + \frac{1}{\varepsilon}W(1-(u_L+u_S)))dx \\ &+ \frac{\sigma_S}{2}\int_Q (\frac{\varepsilon}{2}|\nabla u_S|^2 + \frac{1}{\varepsilon}W(u_S))dx.\end{aligned}$$

Notice that its L^2-gradient satisfies

$$\nabla_{L^2}\tilde{P}_\varepsilon(u_L) = \frac{\sigma_{SL}}{2}[-\varepsilon\Delta u_L + \frac{1}{\varepsilon}W'(u_L)] + \frac{\sigma_V}{2}\varepsilon R_{u_S}(u_L)$$

where the first term

$$\frac{\sigma_{SL}}{2}[-\varepsilon\Delta u_L + \frac{1}{\varepsilon}W'(u_L)],$$

is a classical Allen-Cahn term and the second term

$$R_{u_S}(u_L) = -\left[\Delta u_S + \frac{1}{\varepsilon^2}(W'(u_L) + W'(1-(u_L+u_S))\right],$$

appears as a smooth penalization term which is active only on the boundary of Ω_S.

Finally, incorporating mobilities leads us to consider the following Cahn–Hilliard models:

- **M-CH model**

$$\begin{cases}\partial_t u_L &= \operatorname{div}\left(M(u_k)\nabla(\sigma_{LV}/2\mu_L + \sigma_V R_{u_S}(u_L))\right) \\ \mu_L &= \frac{W'(u_L)}{\varepsilon^2} - \Delta u_L\end{cases}$$

- **NMN-CH model**

$$\begin{cases}\partial_t u_L &= N(u_L)\operatorname{div}\left(M(u_L)\nabla(N(u_L)\left(\sigma_{LV}/2\mu_L + \sigma_V R_{u_S}(u_L)\right))\right) \\ \mu_L &= \frac{W'(u_L)}{\varepsilon^2} - \Delta u_L\end{cases}$$

Note that in practice, we will only use here the **NMN-CH** model for our simulations because the wetting of a thin structure requires to have a model as precise as possible.

Regarding the numerical scheme, the idea is to apply the previous scheme with an explicit treatment of the penalization term $R_{u_S}(u_L)$.

Notice also that the penalization term $R_{u_S}(u_L)$ is active on the whole boundary of Ω_S. In particular, when $u_L = 0$ this term is still active and can be important as it corresponds to the Allen-Cahn term associated to u_S:

$$R_{u_S}(u_L) = -\left(\Delta u_S + \frac{1}{\varepsilon^2}W'(1-u_S)\right) = -\Delta u_S - \frac{1}{\varepsilon^2}W'(u_S).$$

In practice, we propose to localize it only at the liquid phase boundary u_L, which can be done by considering the following variant

$$\tilde{R}_{u_S}(u_L) = R_{u_S}(u_L)\frac{\sqrt{2W(u_L)}}{\sqrt{2W(u_L)+\varepsilon}}.$$

This variant is interesting for it contributes to stabilizing the numerical scheme without disturbing the evolution of the liquid phase.

4.2. **Influence of the surface tension coefficients.** We now propose a numerical experiment in dimension 3 where the initial set is a thin tube. The numerical parameters are given by $N = 2^8$, $\varepsilon = 1/N$, $\delta_t = \varepsilon^4$, $\alpha = 2$, $m = 1$, and $\beta = 2/\varepsilon^2$. We plot on each image of Figure 6 the solution $\mathbf{u}$ calculated at different times t where the solid and liquid phase boundaries are plotted in red and gold, respectively. As in the 2D case, surface tension coefficients have a considerable influence on the evolution of the liquid phase. They affect both the wetting rate and the final shape of the liquid phase.

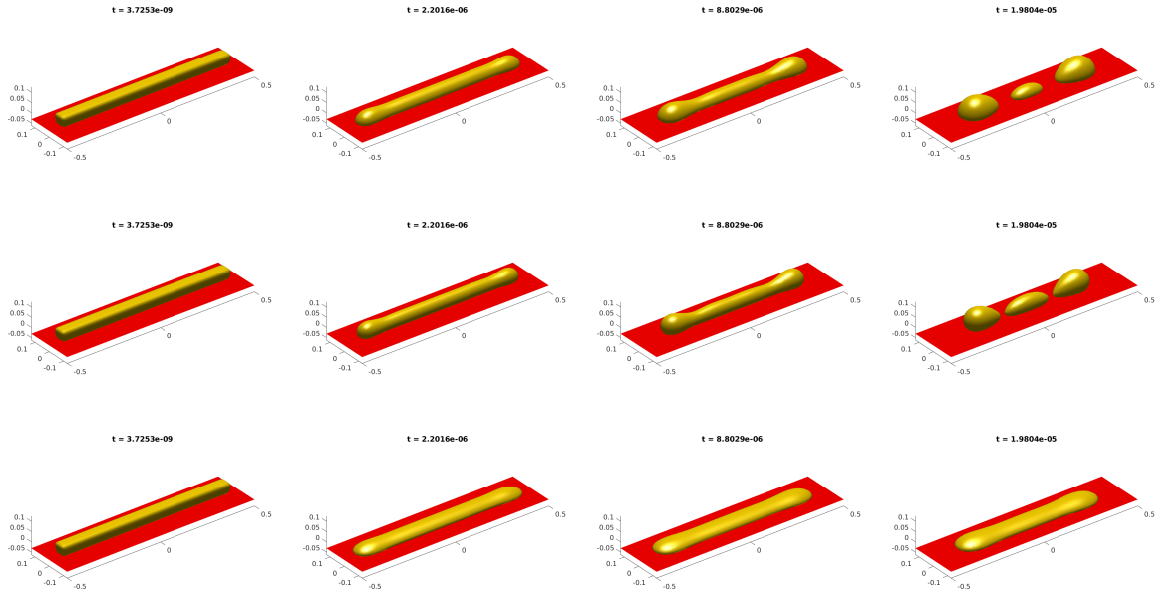

FIGURE 6. Influence of the surface tension coefficients using the **NMN-CH** model: evolution of $\mathbf{u}$ along the iterations; first line using $\sigma_{LV} = \sigma_{VS} = \sigma_{SL} = 1$; second line using $\sigma_{LS} = 1.7$ and $\sigma_{LV} = \sigma_{VS} = 1$; third line, using $\sigma_{VS} = 1.7$, and $\sigma_{LV} = \sigma_{LS} = 1$.

4.3. **Influence of the roughness of the solid support.** Our approach is also well suited for handling solid supports with roughness, i.e., notably difficult configurations for the simulation of wetting. In Figure 7, we test the case of a classical flat support, a support with a randomly generated roughness, and an oscillating support. We observe a direct influence of the substrate roughness on the wetting dynamics, each simulation being initialized in a similar way and using the same set of coefficients.

Acknowledgements The authors acknowledge support from the French National Research Agency (ANR) under grants ANR-18-CE05-0017 (project BEEP) and ANR-19-CE01-0009-01 (project MIMESIS-3D). Part of this work was also supported by the LABEX MILYON (ANR-10-LABX-0070) of Université de Lyon, within the program "Investissements d'Avenir" (ANR-11-IDEX- 0007) operated by the French National Research Agency (ANR).

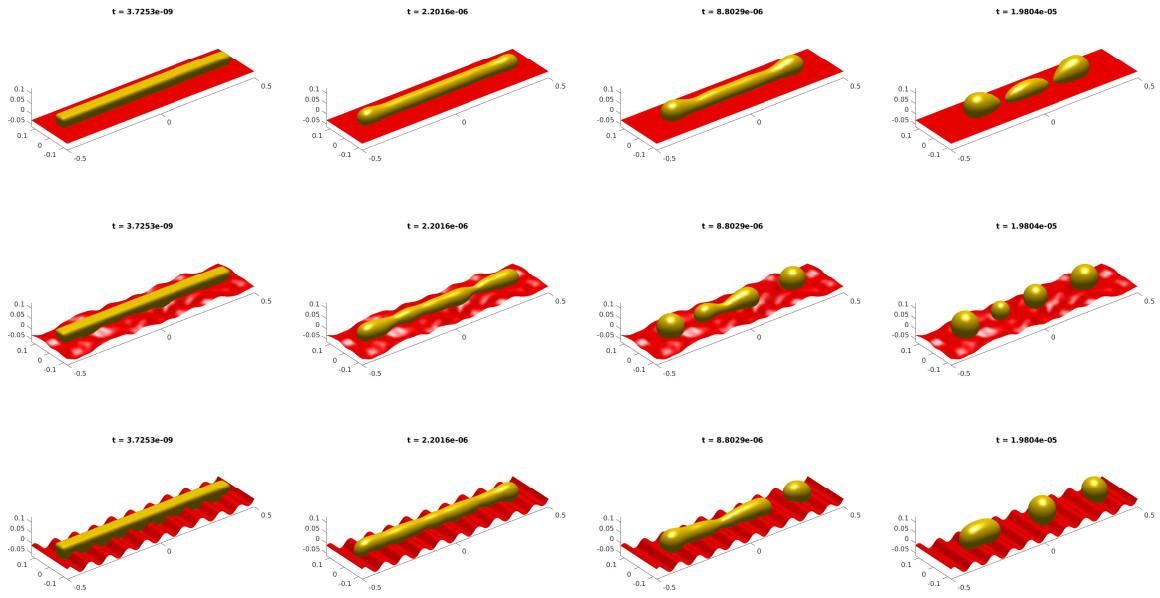

FIGURE 7. Influence of the roughness of the solid support using the **NMN-CH** model: evolution of $\mathbf{u}$ along the iterations using $\sigma_{LS} = 1.7$ and $\sigma_{LV} = \sigma_{VS} = 1$.

CONFLICT OF INTEREST

The authors declare that they have no conflict of interest.

UNIV LYON, INSA DE LYON, CNRS UMR 5208, INSTITUT CAMILLE JORDAN, 20 AVENUE ALBERT EINSTEIN, F-69621 VILLEURBANNE, FRANCE, ELIE.BRETIN@INSA-LYON.FR

UNIV LYON, UNIVERSITÉ CLAUDE BERNARD LYON 1, CNRS UMR 5208, INSTITUT CAMILLE JORDAN, 43 BOULEVARD DU 11 NOVEMBRE 1918, F-69622 VILLEURBANNE, FRANCE, DENIS@MATH.UNIV-LYON1.FR

UNIV LYON, UNIVERSITÉ CLAUDE BERNARD LYON 1, CNRS UMR 5208, INSTITUT CAMILLE JORDAN, 43 BOULEVARD DU 11 NOVEMBRE 1918, F-69622 VILLEURBANNE, FRANCE, MASNOU@MATH.UNIV-LYON1.FR

UNIV LYON, UNIVERSITÉ CLAUDE BERNARD LYON 1, CNRS UMR 5208, INSTITUT CAMILLE JORDAN, 43 BOULEVARD DU 11 NOVEMBRE 1918, F-69622 VILLEURBANNE, FRANCE, SENGERS@MATH.UNIV-LYON1.FR

UNIV LYON, UNIVERSITÉ CLAUDE BERNARD LYON 1, CNRS UMR 5208, INSTITUT CAMILLE JORDAN, 43 BOULEVARD DU 11 NOVEMBRE 1918, F-69622 VILLEURBANNE, FRANCE, TERII@MATH.UNIV-LYON1.FR